Studying the role of DNA-PK in transformation

of breast epithelial cells

A Thesis submitted to

Indian Institute of Science Education and Research Pune

in partial fulfillment of the requirements for the

BS-MS Dual Degree Programme

By

Faseela.E.E

(20131071)

IISER PUNE

Supervisor:
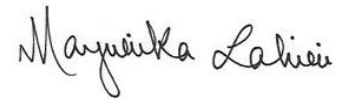
Dr. Mayurika Lahiri,

IISER Pune

Thesis Advisory Committee Member

Prof. LS Shashidhara,

IISER Pune

Certificate

This is to certify that this dissertation entitled '**Studying the role of DNA-PK in transformation of breast epithelial cells'** towards the partial fulfilment of the BS-MS dual degree programme at the Indian Institute of Science Education and Research (IISER), Pune represents study/work carried out by **Faseela E E** at IISER Pune under the supervision of **Dr. Mayurika Lahiri**, Associate Professor, Biology Division, IISER Pune during the academic year 2017-2018.
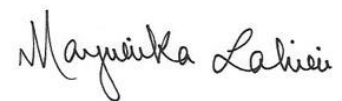
Dr. Mayurika Lahiri
Associate Professor
Biology Division, IISER Pune

Faseela E E
20131071
BS-MS Dual Degree Student
IISER Pune

Declaration

I hereby declare that the matter embodied in the thesis entitled '**Studying the role of DNA-PK in transformation of breast epithelial cells'** are the results of the work carried out by me at the Department of Biology, IISER Pune, under the supervision of **Dr. Mayurika Lahiri**, Associate Professor, Biology Division, IISER Pune and the same has not been submitted elsewhere for any other degree.

Dr. Mayurika Lahiri
Associate Professor
Biology Division, IISER Pune

Faseela E E
20131071
BS-MS Dual Degree Student
IISER Pune

Abstract

DNA alkylating agents are one of the most common DNA damaging agents that we encounter and widely used in cancer chemotherapy. The greatest limitation of such drugs is they can often induce carcinogenic mutations. Methylnitrosourea (MNU) is a monofunctional DNA methylating agent that acts as a mutagen as well as potential carcinogen by forming O^6-methyl Guanine (O^6MeG) adducts in the DNA. Studies in the lab demonstrated that MNU triggers transformation and Golgi dispersal in non-tumorigenic breast epithelial cells (MCF10A) through activation of DNA-dependent protein kinase (DNA-PK). DNA-PK is a major player involved in double-strand DNA break repair through Non-homologous End Joining (NHEJ), it is known to be upregulated in most of the cancers. DNA-PK transcript analysis in breast cancer patients using The Cancer Genome Atlas (TCGA) database also showed an increased RNA expression in tumors compared to adjacent normal. Moreover, Survival analysis of breast cancer patients expressing high level of DNA-PK showed a low survival chance implicating that DNA-PK may have a role in breast cancer. We have also observed DNA-PK activation and aberrant Golgi phenotypes in various breast cancer cell lines such as MCF10AT1, MCF10CA1a, MCF7 and T47D. Here we are investigating the role of DNA-PK in breast epithelial cell transformation and Golgi dispersal. To check for MNU induced transformation of MCF10A on a DNA-PK null background, a stable knockdown cell line will be generated which will help to investigate the role of DNA-PK in transformation. Also, we will be knocking down DNA-PK in already transformed breast epithelial cells to identify whether the cellular transformation and aberrant Golgi phenotypes are DNA-PK dependent.

Table of Contents

List of Figures

List of Tables

List of Abbreviations

ATM   ataxia-telangiectasia mutated

ATR   ATM and Rad3 related

DDR   DNA Damage Response

DMNB   4,5-Dimethoxy-2-nitrobenzaldehyde

DMSO   Dimethyl sulfoxide

DNA-PKcs   DNA-dependent Protein Kinase catalytic subunit

DSB   Double Strand Breaks

EMT   Epithelial to Mesenchymal Transition

ER   Estrogen Receptor

FBS   Fetal Bovine Serum

Her2   Human Epidermal growth factor Receptor 2

HR   Homologous Recombination

KM   Kaplan Meier

MNU   N-methyl -N- nitrosourea

NHEJ   Non-Homologous End Joining

O^6MeG O^6-methylGuanine

PBS   Phosphate Saline Buffer

PCR   Polymerase Chain Reaction

PI3K   Phospho inositol-3- kinase

PR   Progesterone Receptor

PVDF   Polyvinylidene difluoride

RT   Room Temperature

SDS-PAGE   Sodium Dodecyl Sulfate-Polyacrylamide Gel Electrophoresis

shRNA   Small/short hairpin RNA

S_N1 First order nucleophilic substitution

S_N2 Second order nucleophilic substitution

SSB   Single Strand Breaks

TCGA   The Cancer Genome Atlas

TBS-T   Tris Salined Buffer-Tween 20

Acknowledgments

Past five years at IISER Pune was indeed a beautiful journey and the final year made it even more exciting and memorable. It would not have been possible without the help of many individuals whom I wish to acknowledge.

Foremost, I would like to express my sincere gratitude towards my supervisor **Dr. Mayurika Lahiri** for giving me an opportunity to work in her research lab for past three years and continuous guidance and support throughout my project. I would always appreciate her patience and constant faith in my lab work after a lot of failed experiments. I would also like to thank **Prof. L. S Shashidhara** for being my TAC member and for his assistance.

I would like to extend my thanks and love to the awesome lab members of Lahiri lab who made my research experiences amazing. I am grateful to each one of them for spending their valuable time and in one way or another they have contributed to the completion of this thesis. Each one had helped me throughout the period of work, especially during those hard times. I am thankful to **Rupa**, the one I can just hug and cry during difficult times, who is a great research guide and the best mental supporter for everything. Thanks to **Rintu** for her constant help and assistance with the experiments since the day I joined the lab and for inspiring me with motivational stories. I thank **Abhijith**, my brother, who has been supportive in every way, for helping me throughout the period especially with the TCGA. Thanks to **Aishwarya** for all the suggestions and assistance with the experiments particularly with the microscopy. I want to thank **Bhagyashree** for her valuable suggestion with the experiments and Ph.D. applications as well. I thank **Virender**, the one I can always physically fight with and **Vandana** whom I can always verbally fight with, for making the lab environment fun, exciting and interesting. Thanks to **Vaishali** for her encouragement during those tough times, for valuable suggestion and discussions.

Special mention goes to **Kezia**, my twin, for being there for me since the day I came to IISER. She has always been supportive and helpful inside and outside the lab. I acknowledge past Lahiri lab members **Libi** and **Ashiq** for all the help and support throughout the period even after they left the lab, which cannot be forgotten. I also want to thank other lab members **Pradnya** and **Nazneen**.

Introduction:

<u>Biological responses to DNA damage</u>

An accurate transmission of genetic information from parent cell to its daughter cells is essential for the survival of an organism. However, cells are always under the threat of various endogenous and exogenous DNA damaging agents that induce genomic instability and mutations (Norbury and Hickson 2001). In order to monitor and deal with such damages, cells are equipped with a multistep cascade mechanism known as DNA Damage Response (DDR) (Ghosal and Chen 2013). DDR involves a well-organized and highly coordinated network of proteins comprised of sensors, mediators, transducers and effectors (**Figure 1**). The cascade is initiated by sensor kinases which directly recognize the aberrant DNA structures. ATM (ataxia-telangiectasia mutated), ATR (ATM and Rad3 related) and DNA-PKcs (DNA-dependent Protein Kinase catalytic subunit) are the upstream kinases that are present in DDR (Lovejoy and Cortez 2009).
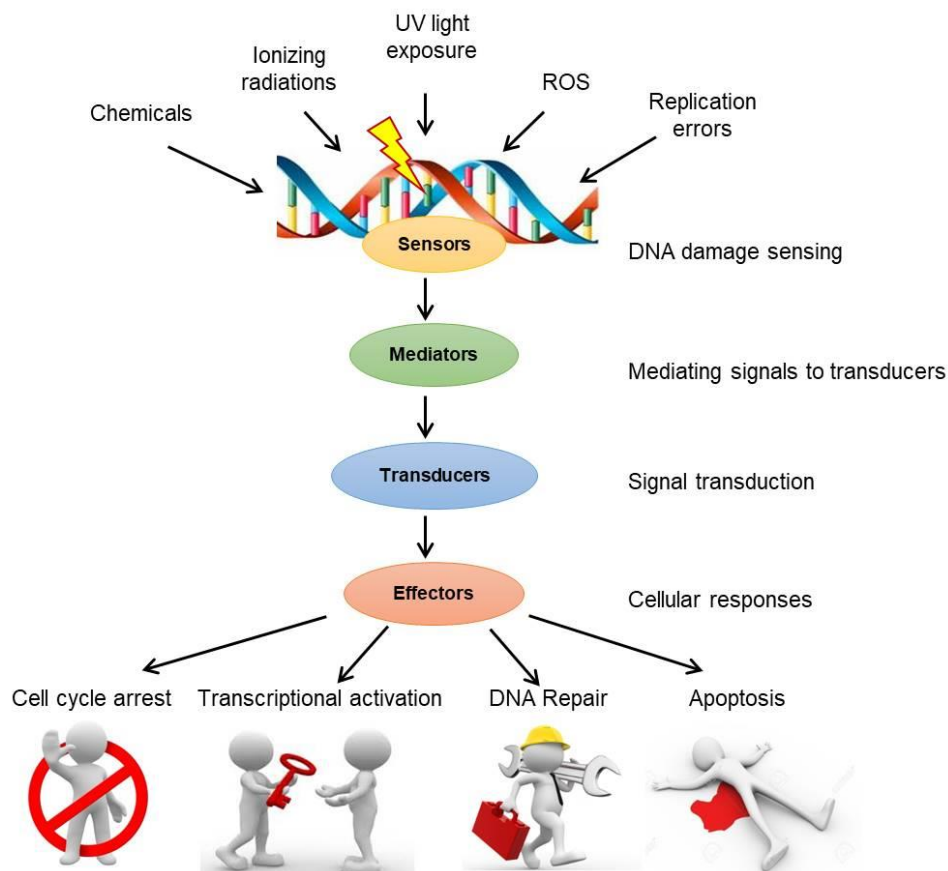

Figure 1: Schematic representation of DNA Damage Response (DDR) Pathway.

ATM and ATR initiate the signaling cascade by phosphorylation of hundreds of downstream proteins, while DNA-PKcs predominantly plays a role in repair of DNA double-strand breaks (DSBs) (Stokes, Rush et al. 2007), (Matsuoka, Huang et al. 1998). ATM and ATR activate downstream checkpoint kinases Chk1 (checkpoint kinase1) and Chk2 (checkpoint kinase2) respectively, through mediator proteins (Abraham 2001). Checkpoint kinases are the transducers which help in amplifying the DNA damage signal. Eventually, the effector proteins receive the signal from transducers and execute cellular responses which include cell cycle arrest, DNA repair and transcriptional activation (Marechal and Zou 2013). When the damage is severe, and above a threshold of repair then the cell undergoes apoptosis. Defects in repair or apoptotic pathway result in genomic instability which can ultimately lead to uncontrolled cell proliferation and cancer (Zhou and Elledge 2000).

DNA damage induced by alkylating agents

DNA alkylating agents are reactive chemicals that transfer alkyl groups to the DNA, thereby disrupting its structure and function and finally leading to cell death (Warwick 1963). They rely on the ability to covalently crosslink the DNA at various positions in the nitrogen base, between the strands or/and within the strands and thus leading to abnormal base pairing and inhibition of cell division (Chaney and Sancar 1996). The N7 position of guanine is the most preferred site for many of the alkylating agents due to its high nucleophilicity (Gates 2009). There are two types of alkylating agents namely S_N1 (first order nucleophilic substitution) and S_N2 (second order nucleophilic substitution), based on the reaction mechanism towards the DNA substrate. S_N1 alkylating agents are able to react directly with the DNA, while S_N2 are those which form a reactive intermediate first and then act on DNA (Fu, Calvo et al. 2012). Alkylating agents can also be classified as monofunctional and bifunctional based on the number of reactive groups present. Monofunctional agents bind and react to a single site on the DNA whereas a bifunctional agent can react with both strands of a DNA, forming an inter-strand crosslink. Alkylating agents can arise exogenously from constituents of air, water and food, tobacco smoke, fuel combustion products and other pollutants and endogenously from by-products of oxidative damage and cellular methyl donors (Hamilton, McRoberts et al. 2003).

Alkylating agents constitute a major class of chemotherapeutic drugs used in cancer treatment with the goal of inducing DNA damage and killing cancer cells (Damia and D'Incalci 1998). However, most of these chemotherapeutic agents can also induce carcinogenic mutations in healthy cells and may lead to the formation of new cancers (Kastan 2008).

MNU-induced DNA damage

N-methyl-*N*-nitrosourea (MNU or NMU) is a monofunctional alkylating agent that reacts through a S_N1 mechanism (Tsubura, Yoshizawa et al. 2010). MNU acts by transferring its methyl group to O^6 group of guanine and forms O^6-methylguanine (O^6-MeG) lesion. When left unrepaired, O^6-MeG pairs with Thymine (T) during replication and further round of replications result in a G:C to A:T transition mutation (**Figure2**) (Margison and Santibanez-Koref 2002). Moreover, MNU can induce both single and double-stranded DNA breaks (Menke, Meister et al. 2000). MNU has also been shown to induce mutational activation of K-Ras oncogene in mouse lymphoma and N-Ras in rat mammary tumors (Corominas, Perucho et al. 1991), (Zarbl, Sukumar et al. 1985). Various other studies imply the role of MNU in cancers in animal models including thymic lymphomas, leukemias, gastrointestinal tumors, brain tumors and mammary tumors (Reese, Allay et al. 2001) (Cox and Irving 1976) (Qin, Zhou et al. 1999).
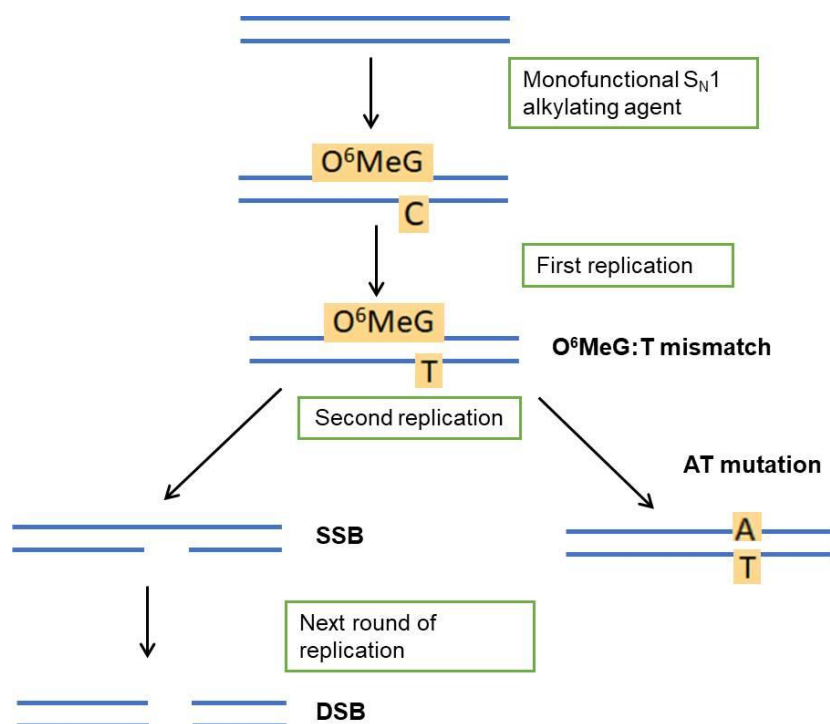
Figure 2: Schematic representation of monofunctional SN1 alkylating agents inducing mutations and double-stranded DNA breaks

Studies from our lab report that MNU induces transformation of non-tumorigenic breast epithelial cells (MCF10A) upon activation of DNA-PKcs. MCF10A cells grown in 3D in presence of MNU showed polarity disruption, EMT like phenotypes, invasion and anchorage-independent growth. Chemical inhibition of DNA-PKcs using DMNB (4,5-Dimethoxy-2-nitrobenzaldehyde) in MNU treated cells showed a reversal of transformation phenotypes (Anandi, Chakravarty et al. 2017).

DNA-dependent Protein Kinase (DNA-PK)

Among various DNA lesions, DSBs are the most deleterious form of DNA damage since misrepaired or unrepaired DSBs may lead to cancer. Non-Homologous End Joining (NHEJ) and Homologous Recombination (HR) are the two essential pathways involved in DSB repair (Mladenov, Magin et al. 2013). HR pathway is restricted to S and G2 phases of cell cycle due to its prerequisite of template strand which is provided by homologous DNA. On the other hand, NHEJ pathway mediates ligation of DSBs without a template strand and thus functions throughout the cell cycle (Weterings and Chen 2008). Compared to HR, NHEJ is less accurate and more error-prone (Takahashi, Kubo et al. 2014).

The NHEJ pathway comprises of DNA-PK, Ligase IV, XRCC4, Artemis and XLF. The central player of NHEJ pathway is the DNA-PK (DNA-dependent protein kinase) holoenzyme which is a complex of three proteins namely DNA-PKcs, Ku70, and Ku80 (Burma, Chen et al. 2006). DNA-PKcs, the catalytic subunit of the complex is the main functional component, while Ku70/ Ku80 proteins are the accessory binding proteins. Ku proteins are necessary and essential for the activation and functioning of DNA-PKcs (Hefferin and Tomkinson 2005). NHEJ is initiated by recognition of DNA DSBs via Ku proteins and binding of Ku heterodimer at the free DNA end in a sequence-independent manner. Ku heterodimer associates with DNA-PKcs to form the active DNA-PK holoenzyme at the site of damage (**Figure 3**). Further downstream proteins including XRCC4 (X-ray cross-complementing protein 4), DNA Ligase IV, XLF (XRCC4-like factor) are recruited at the lesion site, and the processed DNA ends are ligated (Davis and Chen 2013).
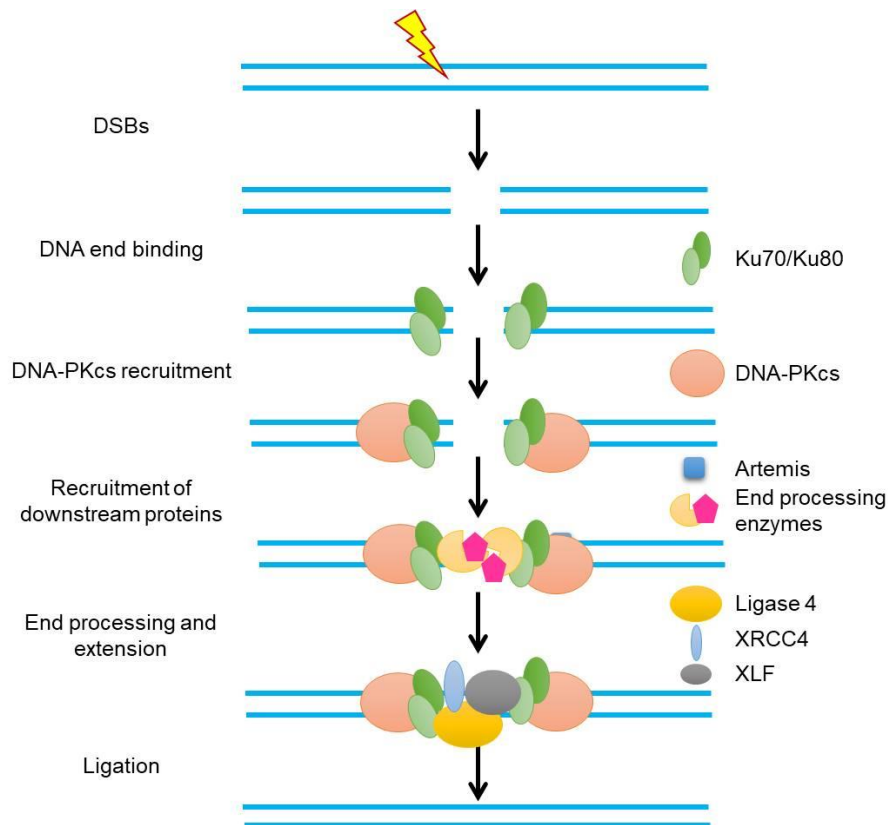
Figure 3: Non-homologous end joining (NHEJ) of DNA double-strand break (DSB) repair.

DNA-PK in cancer

Beyond DNA repair, DNA-PKcs has several other functions such as VDJ recombination of T cell receptor and immunoglobulin genes, telomere length maintenance, cell cycle arrest, transcriptional regulation, modulation of chromatin structure and inflammatory response (Lee and Kim 2002), (Hazra, Mukherjee et al. 2017), (Smith and Jackson 1999), (Burma, Chen et al. 2006). Overexpression of DNA-PKcs has been reported in various cancers including prostate cancer, cervical cancer and oral squamous cell carcinoma (Shintani, Mihara et al. 2003), (Um, Kwon et al. 2004), (Beskow, Skikuniene et al. 2009), (Bouchaert, Guerif et al. 2012). DNA-PKcs has also been identified as a potent driver for tumor progression and metastasis because of its ability to modulate the tumor microenvironment (Kotula, Berthault et al. 2015). Moreover, DNA-PKcs is a potential target for therapeutic interventions for a number of cancer types (Goodwin and Knudsen 2014), (Goodwin, Kothari et al. 2015).

Though there are relevant studies on DNA-PK that associates its role in several cancers, the exact function in each type of cancer is not well understood. Very few studies link DNA-PK to breast cancer, which is the most common cancer worldwide and the primary cause of cancer death in women (Torre, Bray et al. 2015). Two independent studies have shown that targeting DNA-PK sensitizes therapeutically induced DSBs in breast cancer cells, suggesting its significance in cancer treatment (Ciszewski, Tavecchio et al. 2014), (Kim, Park et al. 2002). As previously mentioned, studies in the lab also demonstrated that DNA-PK contributes to transformation of non-tumorigenic cell line upon MNU-induced DNA damage.

We have analyzed the RNA expression profile of DNA-PK in breast cancer based on clinicopathological parameters such as receptor statuses, tumor subtypes, and stages of cancer, using the RNA-Seq dataset from The Cancer Genome Atlas (TCGA). TCGA database provides the gene expression profiling in 33 types of cancers and it may serve as a tool to understand the cancer biomarkers. It is important to note that mRNA levels may not necessarily correlate with protein expression.

DNA-PK mediated Golgi dispersal

DNA damage response is intensely studied with regard to nuclear effects such as cell cycle arrest, DNA repair and transcriptional activation of genes. However not much is known about the cytoplasmic organelle regulation following DNA damage. In response to DNA damage, Golgi reorganizes by fragmentation and dispersal through activation of DNA-PK/GOLPH3/MYO18A pathway. DNA-PK directly phosphorylates GOLPH3 leading to enhanced interaction with MYO18A which results in a dramatic reorganization of Golgi (Farber-Katz, Dippold et al. 2014). Similar studies in the lab also showed DNA-PK mediated Golgi dispersal following MNU induced DNA damage (Anandi, Chakravarty et al. 2017).

Aim:

The specific aim of this study is to identify the role of DNA-PK in initiation and progression of breast cancer, which will be carried out by downregulating DNA-PK in non-tumorigenic cells (MCF10A) treated with MNU and in transformed breast epithelial cells that has high level of DNA-PK.

To knockdown DNA-PK, a short hairpin RNA (shRNA) targeting DNA-PKcs will be constructed and a stable cell line will be generated.

Objectives

- *In Silico* analysis of DNA-PK expression profile in breast cancer patients and its association with clinicopathological parameters
- To identify the DNA-PK status Golgi phenotype in various breast cell lines
- To validate MNU-induced transformation of MCF10A cells through DNA-PK following DNA-PKcs knockdown
  - o Cloning of shRNA construct against DNA-PKcs
  - o Generation of stable MCF10A cell line expressing shDNA-PKcs
  - o To check whether MNU induces transformation in DNA-PKcs knockdown background

Materials and Methods

Cloning of shRNA construct against DNA-PKcs into pLKO.1-TRC vector

shRNA oligonucleotides targeted against the Kinase domain of DNA-PKcs (5' GGAGCTTACATGCTAATGTAT 3') were purchased from Integrated DNA Technologies (IDT). The knockdown construct against DNA-PKcs was prepared by annealing of forward and reverse DNA-PK shRNA oligonucleotides by the following reaction mixture and PCR program (**Table 1 and Table 2)** in a thermocycler. Annealed oligonucleotides were run on a 3% gel and annealed bands were extracted using QIAquick Gel Extraction Kit (Qiagen). The quantity of DNA was detected via NanoDrop readings and visual quantification on the gel.

Table 1: Annealing reaction mixture for 10 µl reaction

SI No.	Annealing Reagents	Volume (µl)
1	DNA-PKcs shRNA forward oligo	1.0
2	DNA-PKcs shRNA reverse oligo	1.0
3	10 x T4 DNA Ligase buffer (Takara)	1.0
4	T4 PNK	0.5
5	Nuclease-free water	6.5

Table 2: PCR program for annealing

Temperature	37 °C	95 °C	90 °C	85 °C	80 °C	75 °C	70 °C	65 °C	60 °C	55 °C	50 °C	45 °C	40 °C	35 °C	30 °C	25 °C	4°C
Time	30'	5'	1'	1'	1'	1'	1'	1'	1'	1'	1'	1'	1'	1'	1'	1'	hold

The Plasmid vector (pLKO.1-TRC) was extracted by QIAprep Spin Miniprep Kit (Qiagen). Concentration was checked using NanoDrop readings and quality of DNA was detected by running a 0.8% agarose gel. 3 µg of the pLKO.1-TRC vector was digested with EcoRI Hf (New England Biolabs or NEB) and AgeI Hf (NEB) for 3 hours at 37°C followed by CIP (Calf Intestinal Alkaline Phosphatase; NEB) treatment for 1 hour at 37°C. Digested plasmid was run on a 1% agarose gel at 80 V and band

corresponds to ~7.0 kb was extracted from the gel and purified using QIAquick Gel Extraction Kit (Qiagen). The amount of purified DNA was checked using NanoDrop reading and visual quantification on the gel.

Table 3: Restriction digestion for 50 µl reaction

Sl.No	Digestion Reagents	Volume (µl)
1	DNA	~3µg
2	10x cut smart buffer (NEB)	5
3	AgeI Hf (NEB)	3
4	EcoRI Hf (NEB)	3
5	MilliQ water	Make up to 50 µl

Ligation reaction was carried out at 16°C overnight with a set of vector to insert ratios (1:1, 1:2, 1:3, 1:4, 1:5 and 1:6) and obtained positive colonies only in 1:5 ratio (i.e.,25ng vector + 125ng insert) **(Table 4)**

Table 4: Ligation reaction for 10 µl

Sl No.	Reagents	Vector: insert	1:5 (µl)	-ve control (µl)
1	Digested pLKO.1-TRC		25ng	25ng
2	shDNA-PKcs		125ng	0
3	T4 DNA Ligase (Takara)		1	1
4	10x T4DNA Ligase buffer (Takara)		1	1
5	Milli-Q water		Up to 10 µl	Up to 10 µl

Ligated products were transformed into DH5α *E. coli* chemically competent cells using 5x KCM buffer (500mM KCl, 150mM CaCl2, 250mM MgCl2) and plated on LB-agar plates containing ampicillin (100 µg/ml) and incubated at 30°C for 24 hours. Recombinant plasmids were extracted from obtained colonies and ran on a 0.8% agarose gel to check quality and size of the DNA. These plasmids were screened for successful insertion by digesting with XhoI (**Table 5**) then analyzed the release bands on 2% agarose gel.

Table 5: XhoI digestion for 15 µl reaction

Sl.No	Digestion Reagents	Volume (µl)
1	DNA	0.5- 1µg
2	10x cut smart buffer	1.5
3	XhoI	1
4	MilliQ H_2O	Up to 15

Transfection of shDNA-PKcs in HeLa cells for shRNA mediated knockdown

HeLa cells were seeded at a density of 1×10^6 per 60mm dish or 3.5×10^5 per 35mm dish and incubated at 37°C. Transfection was performed when cells were 60-70% confluent using Lipofectamine reagent as described below: plasmid DNA (4 µg for 60mm dish or 2 µg for 35mm dish) was diluted in serum-free media OptiMEM to make up the volume to 400 µl or 200 µl. Meanwhile, 16 µl or 8µl Lipofectamine per reaction was mixed with OptiMEM to make up a volume of 400 µl or 200 for 60mm dish or 35 mm dish respectively and incubated at room temperature for 5 minutes. Following the 5 minute incubation, Lipofectamine- OptiMEM mix (400 µl or 200 µl) was added to DNA-OptiMEM mix (400 µl or 200 µl) and incubated for 20 minutes at room temperature. In the meantime, cells were incubated with OptiMEM serum-free media for 20 minutes at 37°C. Subsequently, OptiMEM was added to the DNA-Lipofectamine-OptiMEM mix to make up final volume to 4 ml or 2 ml and added to the cells followed by incubation at 37°C for 4 hours. Once the incubation is over 2 ml or 1 ml DMEM complemented with 30% FBS was added to the cells. 18-20 hours after transfection media was replaced by adding DMEM containing10% FBS and incubated at 37°C. After 48 to 72 hours of transfection, cell lysates were collected in 2x Laemmli sample buffer (68.5mM Tris (pH 6.8), DTT, 26.3% (w/v) glycerol, 0.01% Bromophenol blue, 2.1% SDS) 48 hours post-transfection.

Immunoblotting

Cells were washed with PBS, scraped the cells off the plate and then lysed and collected in 2x Laemmli sample buffer (68.5mM Tris (pH 6.8), DTT, 26.3% (w/v) glycerol, 0.01% Bromophenol blue, 2.1% SDS). Cell lysates were pre-heated at 95°C

for 5 minutes and microcentrifuged at 13,400 rpm for 1 minute at RT. samples were separated on 6% Sodium dodecyl sulfate polyacrylamide gel electrophoresis (SDS-PAGE) for DNA-PKcs. It is consist of 30% acrylamide; 20%, 1.5M Tris (pH 8.8); 25, 10% SDS; 1%, 10% Ammonium Persulfate; 1% and TEMED; 0.08%. The gel was resolved at 120 V for 6 hours and transferred onto PVDF (Polyvinylidene difluoride) membrane in 1X transfer buffer (25 mM Trizma base, 192 mM glycine, 10% methanol and 0.01% SDS) at 115 mA for 16 hours followed by fast transfer at 250mA for 3hours at 4°C. The membrane was blocked in 5% skimmed milk (SACO Foods, US) prepared in 1x TBS-T (Tris Buffered Saline-Tween20: 10mM Tris, 15mM NaCl, KCl, 0.05% Tween 20) overnight at 4°C in the rotor. Blots were then incubated with primary antibody (Rabbit anti-DNA-PKcs, Cell Signalling Technology, 1:1,000) for 16-18 hours at 4°C the rotor. Once primary incubation was over, blots were washed three times with 1x TBS-T for 15 minutes and incubated with Horseradish peroxidase (HRP) conjugated secondary antibody solution (anti-Rabbit HRP, Jackson, 1:10,000) prepared in 5% skimmed milk (SACO Foods, US) for 1 hour at RT in the rotor. Blots were further washed thrice with 1x TBS-T and developed using Immobilon Western luminol reagent and peroxide substrate (Millipore). Images were taken using ImageQuant LAS4000 gel documentation system.

To probe for GAPDH and Ku70/80, 10% resolving gel (30% acrylamide; 33%, 1.5M Tris (pH 8.8); 25, 10% SDS; 1%, 10% Ammonium Persulfate; 1% and TEMED; 0.08%) was prepared and transfer was for 3 hours at 250mA. Blocking was carried out either at 4°C, overnight or at RT for I hour. For GAPDH blot was incubated with Rabbit anti-GAPDH (Sigma, 1:4,000) at RT for I hour. To probe for Ku70/80, the blot was incubated with Rabbit anti- Ku70+80 (Abcam, 1:5,000) at RT for I hour. Rest of the processing was same as described above.

Immunofluorescence

5×10^4 HeLa cells (2×10^4 for control cells) were grown on coverslips per 24-well plate and transfected with shDNA-PK using Lipofectamine mediated method as described previously. After 24 hours of transfection cells were treated with 1mM MNU dissolved in DMSO. 24 hours post-MNU treatment, coverslips were rinsed twice with 1X PBS (NaCl, Na_2HPO_4, and NaH_2PO_4) and cells were fixed using freshly prepared 4% formaldehyde prepared in PBS for 20 minutes in the dark at RT.

Then coverslips were washed twice with 1X PBS for 10 minutes and permeabilized using PBS containing 0.5% Triton-X-100 for 10 minutes at 4°C and rinse with 1X PBS-glycine (1X PBS containing 100 mM glycine) once followed by a rinse with 1XPBS for 10 minutes each at RT. Blocking was carried out in 10% HS prepared in 1X IF buffer (10% Sodium azide, BSA, Triton-X-100) for 1 hour at RT. Subsequently, cells were incubated with Mouse anti-phospho-DNA-PKcs (T2609) (Abcam, 1:100) or with Rabbit anti-phospho-DNA-PKcs (S2056) (Abcam, 1:100) and Mouse GM130 (Millipore, 1:100) prepared in 10% HS at 4°C, overnight in a humid chamber. Following day, cells were rinsed thrice with 1x IF buffer for 20 minutes each. Afterward, cells were incubated with Alexa-568 conjugated secondary antibody (anti-mouse/donkey 568, 1:500, Invitrogen) prepared in blocking solution for 1 hour at RT. Wells were washed once with 1X IF buffer for 20 min and twice with 1X PBS for 10 minutes each at RT. To stain the nucleus cells were stained with Hoechst 333258 (1:4000, Invitrogen) prepared in 1X PBS and incubated for 5 minutes at RT. Then cells were rinsed twice with 1X PBS for 10 minutes at RT. Coverslips were mounted on glass slides using mounting medium and sealed with transparent nail polish. Images were captured using 63x oil-immersion objective under Apotome or Leica SP8 microscope.

TCGA analysis

DNA-PK mRNA expressions in breast cancer patient samples were analyzed by using RNA-Seq dataset obtained from The Cancer Genome Atlas (TCGA) (http://cancergenome.nih.gov/). Statistical analyzes were performed by GraphPad Prism software and significance was calculated with non-parametric student's t-test or Kruskal-Wallis test followed by Dunn's post hoc test

Survival analysis

Survival analysis of breast cancer patients expressing high/low DNA-PK was performed by Kaplan Meier survival plot using KM Plotter (Lanczky, Nagy et al. 2016). According to median value expression of DNA-Pkcs, patient samples were split into two groups.

Results and Discussion

In Silico analysis of DNA-PK expression profile in breast cancer

Adjacent normal versus tumor

Several studies have reported that DNA-PK is upregulated in most of the cancers. However there are ambiguous results on DNA-PK in breast cancer. To analyze the DNA-PK expression at mRNA level in breast cancer, we have used the RNA-Seq data set from The Cancer Genome Atlas (TCGA) online database and analyzed using GraphPad Prism software. The transcript level of all three DNA-PK genes i.e., PRKDC (gene encoding DNA-PKcs), XRCC5 (Ku80) and XRCC6 (Ku70) in breast tumors were compared with their adjacent normal issue and the significance test was carried out using non-parametric unpaired t-test (**Figure 4**). DNA-PKcs and Ku80 expressions were significantly high in tumors compared to adjacent normal but not in case of Ku70.
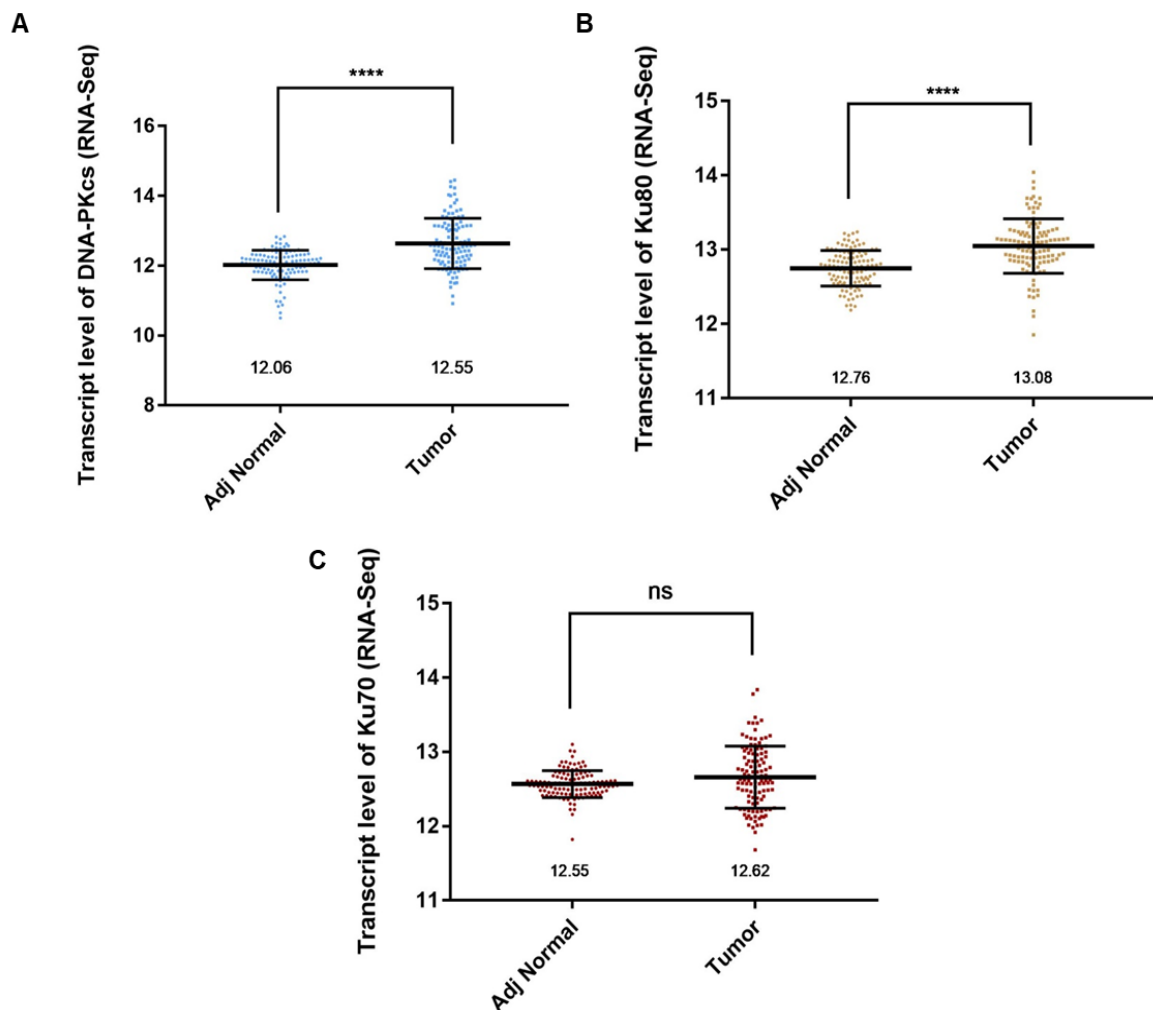
Figure 4: DNA-PK transcript level in Adjacent normal and tumor tissues of breast cancer patients. Transcript level comparison between adjacent normal and tumor for **A)** PRKDC (DNA-PKcs) gene **B)** XRCC5 (Ku80) gene and **C)** XRCC6 (Ku70) gene showing a significantly high mRNA expression of DNA-PKcs **(A)** and Ku80 **(B)** in tumors but not in case of Ku70 **(C)**. The analysis is performed by non-parametric student's t-test using GraphPad Prism. Median values are indicated. ns (non-significant) $P>0.05$, *$P \leq 0.05$, **$P \leq 0.01$, ***$P \leq 0.001$, ****$P \leq 0.0001$

DNA-PK levels based on receptor status

Based on receptor statuses, tumor samples are categorized as Estrogen Receptor positive/negative ($ER^{+/-}$), Progesterone Receptor positive/negative ($PR^{+/-}$) and Human Epidermal growth factor Receptor 2 positive/negative ($Her2^{+/-}$). Using these receptor statuses, breast cancer samples were divided into different subtypes such as Hormone receptor positive and Her2 positive ($ER^{+}PR^{+}Her2^{+}$), Hormone receptor positive and Her2 negative ($ER^{+}PR^{+}Her2^{-}$), Hormone receptor negative and Her2 positive ($ER^{-}PR^{-}Her2^{+}$) and Triple Negative Breast Cancer ($ER^{-}PR^{-}Her2^{-}$). Transcript levels of these subtypes were plotted and compared to the adjacent normal tissue expression and significance was tested by Kruskal-Wallis test followed by Dunn's post hoc test.

DNA-PKcs and Ku 80 transcript levels were significantly high in all the categorized receptor statuses, while Ku70 showed high expression only in $ER^{-}PR^{-}Her2^{+}$ and TNBC compared to adjacent normal (**Figure 5**).
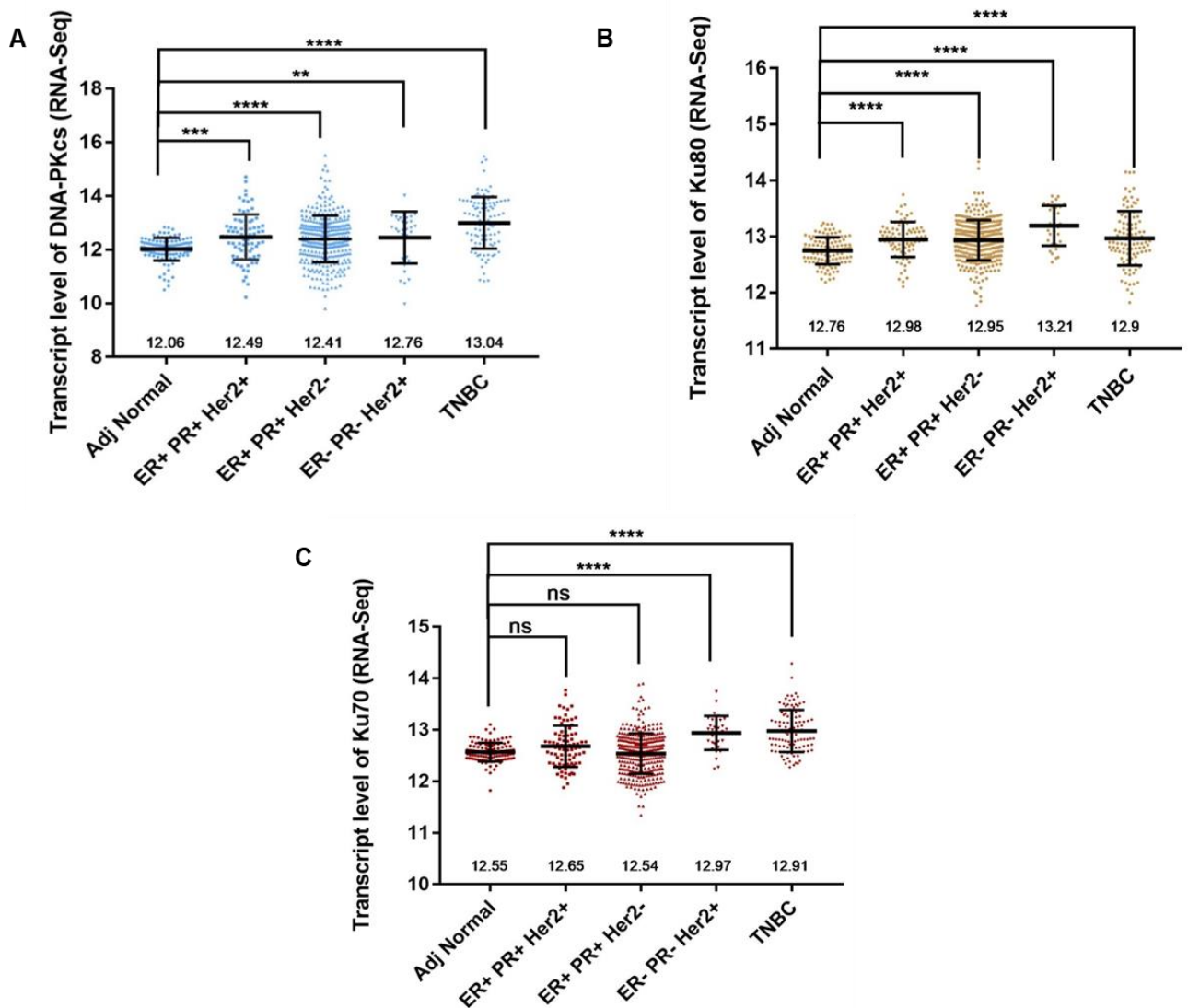
Figure 5: DNA-PK transcript level based on receptor statuses. Transcript level expression of DNA-PK in breast cancer patients for adjacent normal, ER$^+$PR$^+$Her2$^+$, ER$^+$PR$^+$Her2$^-$, ER$^-$PR$^-$Her2$^+$ and TNBC plotted for **A)** PRKDC (DNA-PKcs) gene **B)** XRCC5 (Ku 80) gene and **C)** XRCC6 (Ku 70) gene showing a high level of DNA-PKcs and Ku80 in all the receptor statuses of breast cancer. Significantly high expression of Ku70 was observed only in ER$^-$PR$^-$Her2$^+$ and TNBC. Significance was tested by Kruskal-Wallis test followed by Dunn's post hoc test using GraphPad Prism. ns $P > 0.05$, *$P \leq 0.05$, **$P \leq 0.01$, ***$P \leq 0.001$, ****$P \leq 0.0001$. Median values are shown for each set.

DNA-PK levels across different subtypes

DNA-PK expression levels were checked in various molecular subtypes of breast cancer and compared to their adjacent normal and significance was tested by Kruskal-Wallis test followed by Dunn's post hoc test. Luminal A subtype is ER/PR

positive and Her2 negative with low expression of Ki67 proliferation marker. Luminal B is ER/PR positive while Her2 either positive or negative and high level of Ki67. Her2 enriched is ER/PR negative and Her2 positive while basal like subtype is Triple negative. Normal like is ER and/or PR positive and Her2 negative with low level of Ki67.

DNA-PKcs and Ku 80 transcript levels are significantly high in all the molecular subtypes of breast cancer, whereas Ku70 showed high expression only in Her2^{+} enriched and basal-like subtype compared to adjacent normal (**Figure 6**).
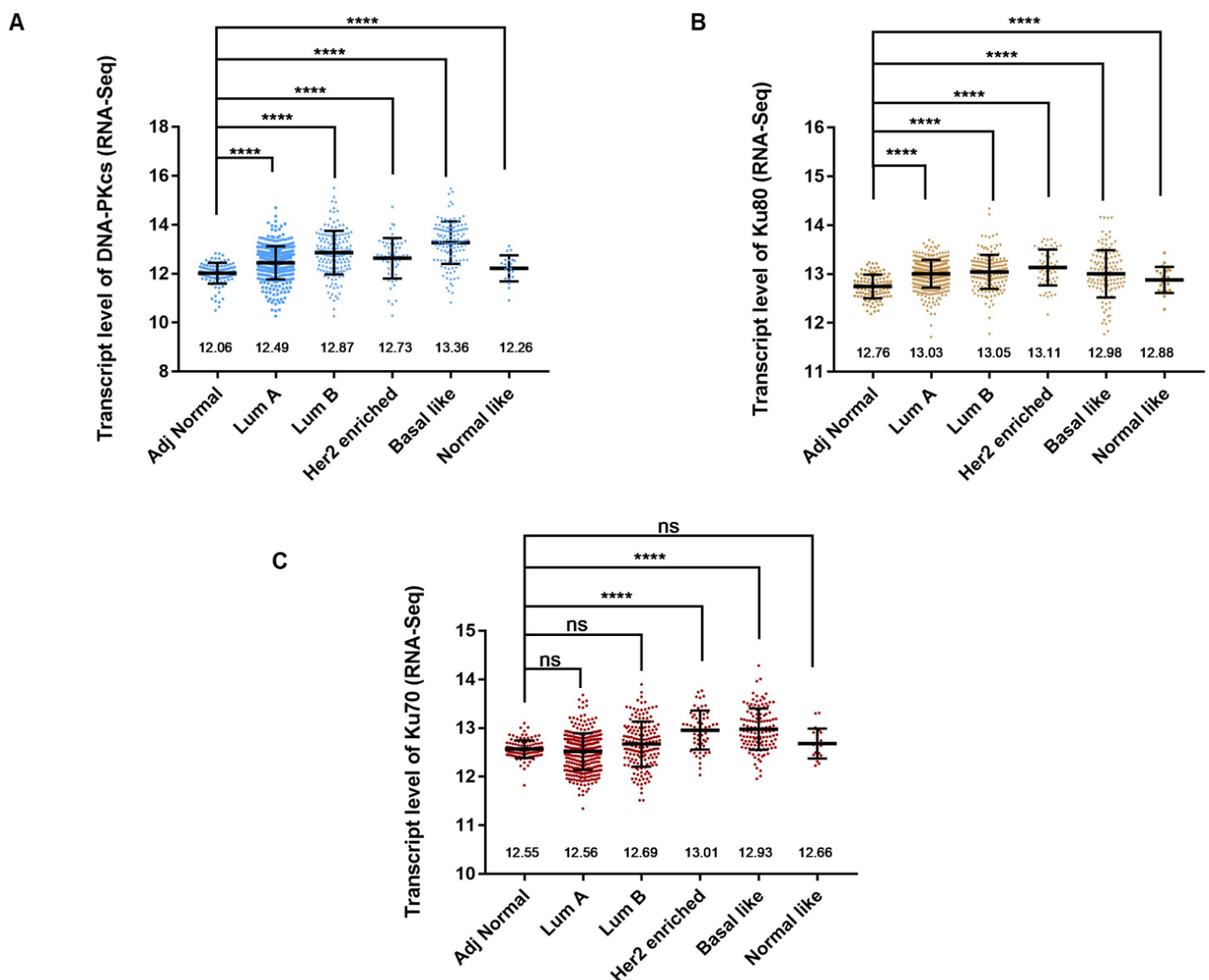

Figure 6: DNA-PK transcript level molecular subtypes. Transcript level expression of DNA-PK in breast cancer patients for adjacent normal, Luminal A, Luminal B, Her2 enriched, Basal-like and Normal-like plotted for **A)** PRKDC (DNA-PKcs) gene **B)** XRCC5 (Ku 80) gene and **C)** XRCC6 (Ku 70) gene. DNA-PKcs and Ku80 transcript levels are high across the molecular subtypes of breast cancer. While Ku70 expression is high in

Her2 enriched and Basal like. Significance was tested by Kruskal-Wallis test followed by Dunn's post hoc test using GraphPad Prism. Median values are shown for each set. ns $P>0.05$, $*P\leq0.05$, $**P\leq0.01$, $***P\leq0.001$, $****P\leq0.0001$.

DNA-PK levels across different stages of breast cancer

Across various stages of breast cancer, DNA-PK expression levels were checked and compared to their adjacent normal and significance was tested by Kruskal-Wallis test followed by Dunn's post hoc test. Based on the size of the tumor, invasiveness, presence in lymph node and metastasis, breast cancer is categorized as stage I, stage II, stage III and stage IV. Stage I describing invasive cancer that remains in the site of origin and Stages IV being the invasive cancer that spread to another part of the body or metastasizes.

DNA-PKcs and Ku80 transcript levels were significantly high in all the stages of breast cancer except for stage IV. On the other hand, Ku70 expression is high in only stage II and Stage III (**Figure 7**).
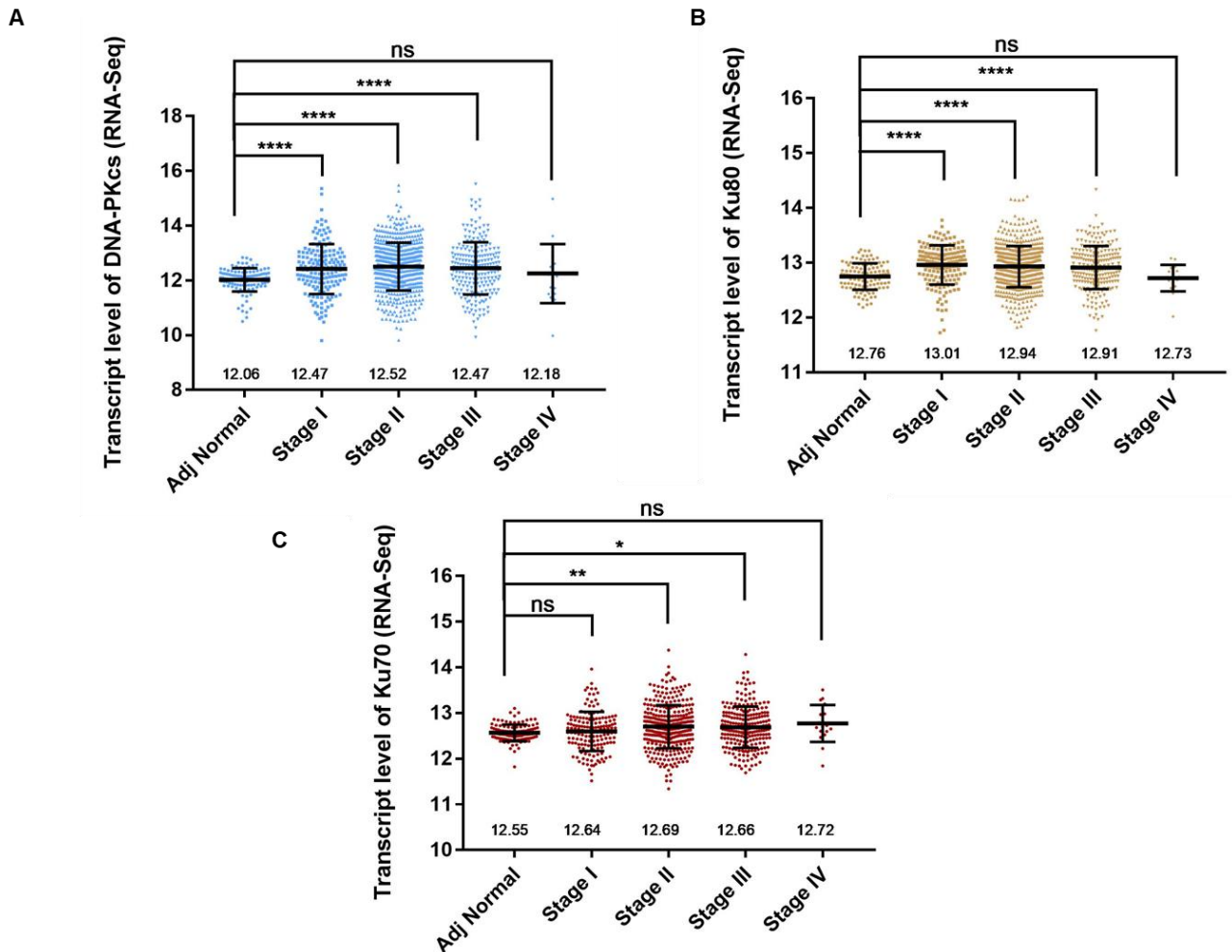
Figure 7: DNA-PK levels across different stages of breast cancer. Transcript level expression of DNA-PK in breast cancer patients across various stages (Stage I, Stage II, Stage III, Stage IV) of breast cancer plotted for **A)** PRKDC (DNA-PKcs) gene **B)** XRCC5 (Ku 80) gene and **C)** XRCC6 (Ku 70) gene. DNA-PKcs and Ku80 levels are high in all stages of breast cancer except stage IV. However Ku70 levels are high only in stage II and III. Significance was tested by Kruskal-Wallis test followed by Dunn's post hoc test using GraphPad Prism. Median values are shown. ns $P > 0.05$, *$P \leq 0.05$, **$P \leq 0.01$, ***$P \leq 0.001$, ****$P \leq 0.0001$.

Survival analysis using KM (Kaplan Meier) plotter

Survival analysis of in breast cancer with respect to DNA-PK expression

From the *In Silico* analysis of DNA-PK expression it is evident that DNA-PKcs, Ku80 and Ku70 transcript levels are high in more aggressive breast cancers. To assess the effect of DNA-PK in survival of breast cancer patients, a survival analysis was

carried out using Kaplan-Meier plot (KM plot). High and low values were set by splitting patients with median value.

Breast cancer patients with high expression of DNA-PKcs (PRKDC) showed a poor survival which is consistent even in ER$^+$PR$^+$Her2$^-$, Luminal A and Basal-like subtype (**Figure 8**). Survival analysis for breast cancer patients expressing high and low levels of Ku80 or Ku70 was carried out using the same portal but showed no significant difference in the patient survival.
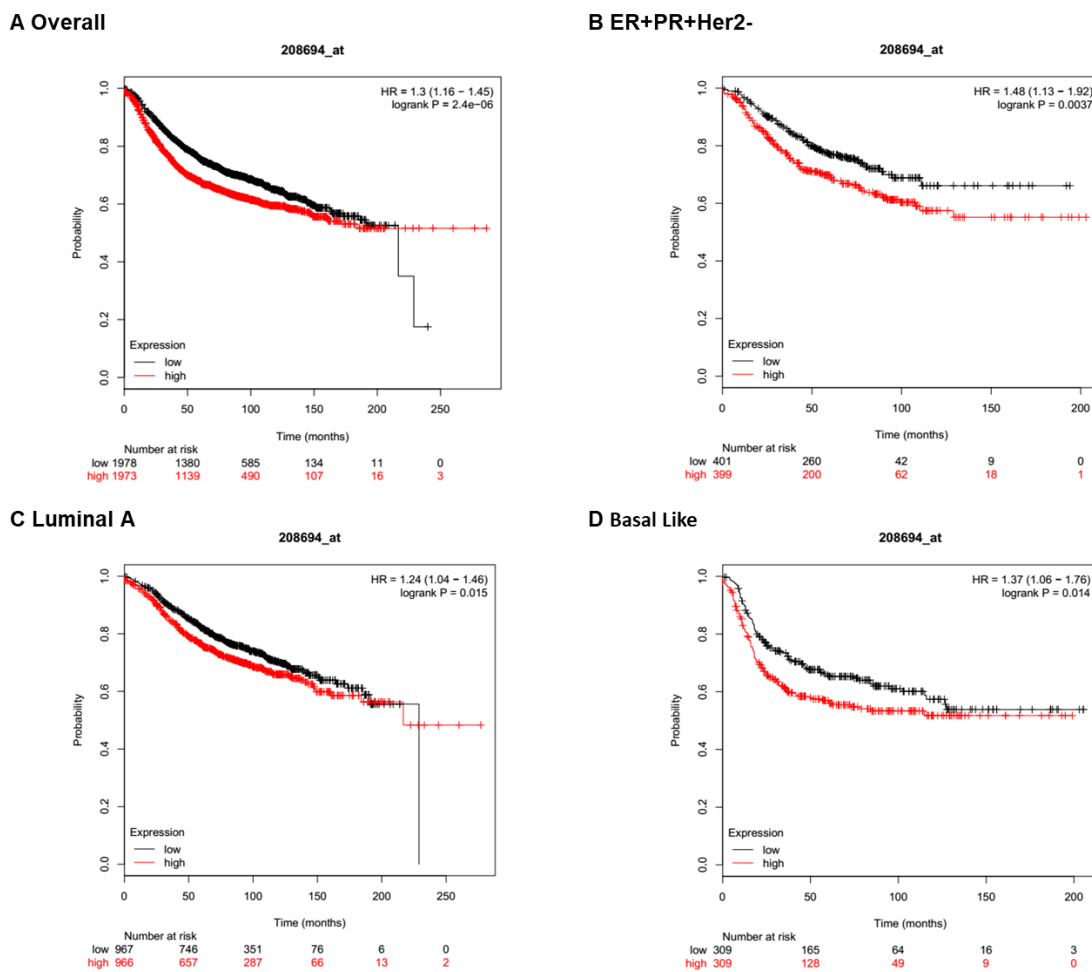

Figure 8: Survival analysis of breast cancer patients expressing DNA-PKcs. Kaplan-Meier plot for disease free survival chance of breast cancer patients of **A)** overall set, **B)** ER$^+$PR$^+$Her2$^-$, **C)** Luminal A subtype and **D)** Basal-like subtype showing a poor survival chance associated with breast cancer patients having high DNA-PKcs.

DNA-PK protein levels in various breast cell lines

From **Figure 4** it is clear that DNA-PKcs and Ku80 mRNA levels are high in breast tumors compared to adjacent normal tissue. But mRNA level does not always correlate with the protein expression. In order to check the expression of DNA-PK proteins in various breast cell lines we have done a western blotting and probed for DNA-PKcs, Ku80 and Ku70 (**Figure 9**). MCF10A is a non-tumorigenic breast epithelial cell line, MCF10AT1 is pre-malignant breast epithelial cell line, MCF10CA1a malignant cell line and MCF7 and T47D are breast cancer cell lines. Ku70, Ku80 and DNA-PKcs levels were observed high in breast cancer cell lines MCF7 and T47D. MCF10A cells treated with 1mM MNU is also showed a high level of Ku70 and Ku80 but not DNA-PKcs. To confirm the trend observed here, we will be repeating this experiment.
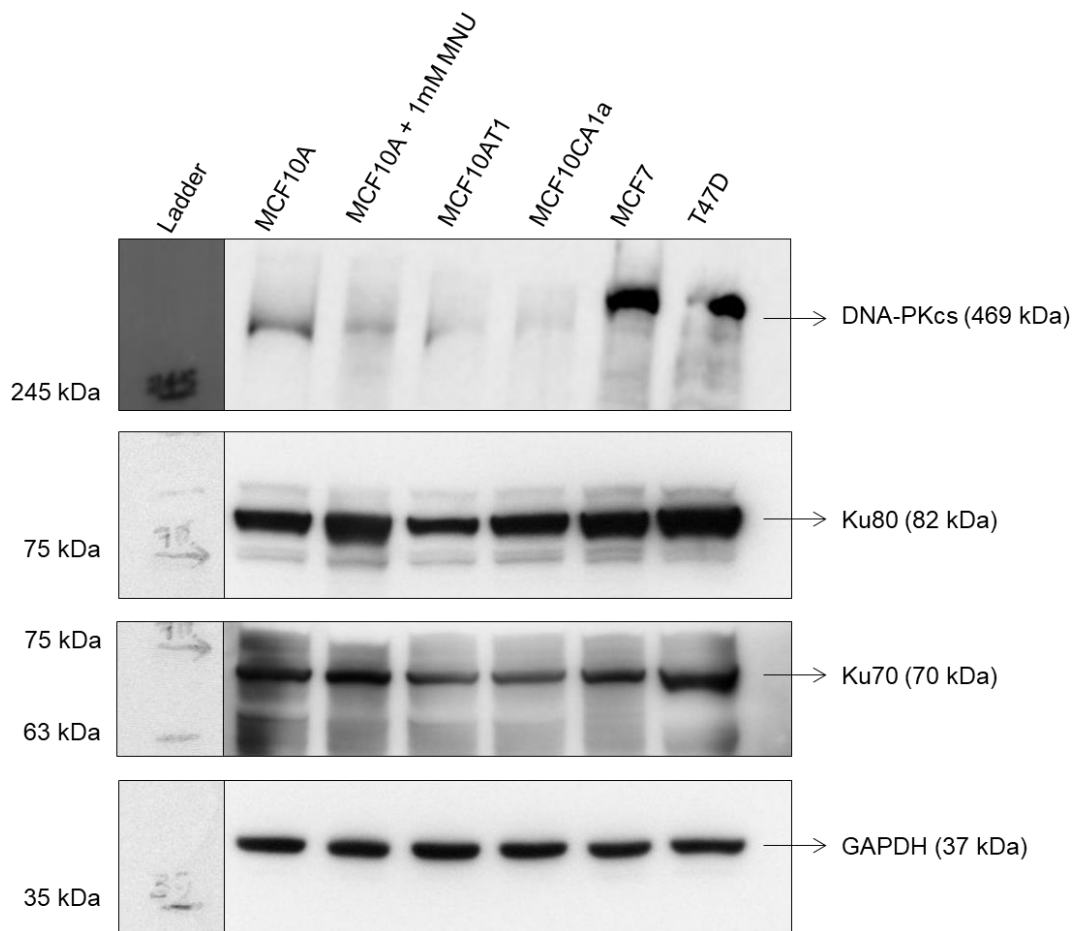

Figure 9: DNA-PK protein levels in various breast cell lines. Western blot image for DNA-PKcs (469kDa), Ku80 (82kDa) and Ku70 (70kDa) proteins in MCF10A,

MCF10A+1mM MNU, MCF10AT1, MCF10CA1a, MCF7 and T47D cells. MCF10A is a non-tumorigenic breast epithelial cell line, MCF10AT1 is pre-malignant breast epithelial cell line, MCF10CA1a malignant cell line while MCF7 and T47D are breast cancer cell lines. Ku70, Ku80 and DNA-PKcs levels were observed high in MCF7 and T47D. MCF10A cells treated with 1mM MNU is also showed a high level of Ku70 and Ku80 but not DNA-PKcs. GAPDH (37 kDa) is used as loading control.

DNA-PK activation and Golgi phenotypes in breast cell lines

As previously mentioned, DNA-PK activation and DNA-PK mediated Golgi dispersal were observed in non-tumorigenic cells (MCF10A) upon MNU induced damage. To check activation of DNA-PK and Golgi morphology in various breast cancer cell lines, we have stained for phospho-DNA-PKcs (S2056) and GM130 (cis Golgi marker) respectively. MCF10A, a non-tumorigenic cells did not show activation of DNA-PKcs while MCF10AT1 (pre-malignant), MCF10CA1a (malignant), MCF7 (breast adinocarcinma) and T47D (invasive ductal carcinoma) cells showed an activation of DNA-PK (**Figure 10A**). A compact Golgi structure was detected in MCF10A whereas aberrant Golgi morphologies were observed in pre-malignant, malignant and breast cancer cells. Compared to MCF10A all other breast cells showed a significantly high Golgi area (**Figure 10B**). To investigate whether this altered Golgi phenotypes are mediated by DNA-PK, we will be looking at Golgi phenotypes after shRNA mediated knockdown.
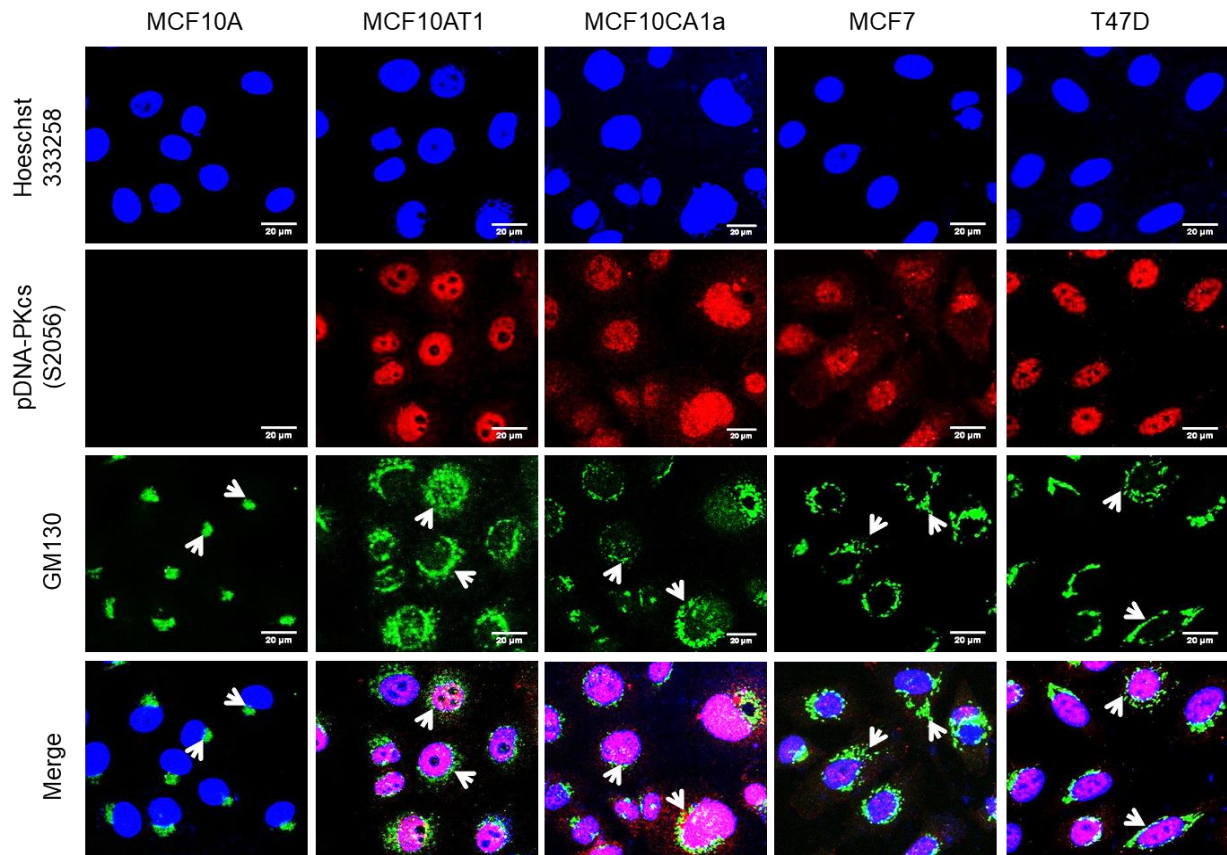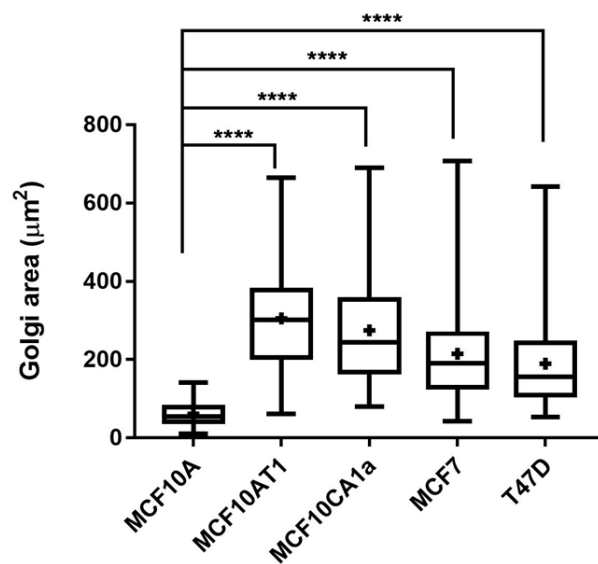
Figure 10: Immunofluorescence image for DNA-PK activation and Golgi phenotypes in various breast cell lines. A) IF image stained for phospho DNA-PKcs (S2056) and GM130 (Golgi marker 130) for MCF10A (non-tumorigenic breast epithelial

cell line), MCF10AT1 (pre-malignant), MCF10CA1a (malignant), MCF7 (breast cancer cell line) and T47D (breast cancer cell line). Excpect MCF10A all other cells showed DNA-PKcs activation at S2056 site. A highly compact Golgi (as marked with arrow) was observed in MCF10A cells while all other cells showed aberrant Golgi. **B)** Quantification for Golgi area compared with MCF10A cells. Significance test was done using one-way ANOVA. ns P>0.05, *P≤0.05, **P≤0.01, ***P≤0.001, ****P≤0.0001. Scale bar 20μm.

<u>shRNA mediated knockdown of DNA-PKcs</u>

Transfection of shDNA-PK.eGFP in HeLa cells

We already had a shRNA against DNA-PK cloned in pLKO.eGFP vector. To test the efficiency of knockdown by the shRNA, we transfected HeLa cells with either shDNA-PK.eGFP (pLKO.eGFP vector containing shRNA construct against DNA-PK) or empty vector pLKO.1.eGFP by the Lipofectamine mediated method. Successful transfection was confirmed by visualization of fluorescence (**Figure 11A**). 24 hours post transfection cells were treated with 1mM of MNU to induce DNA damage and activate DNA-PK (**Figure 11B**).
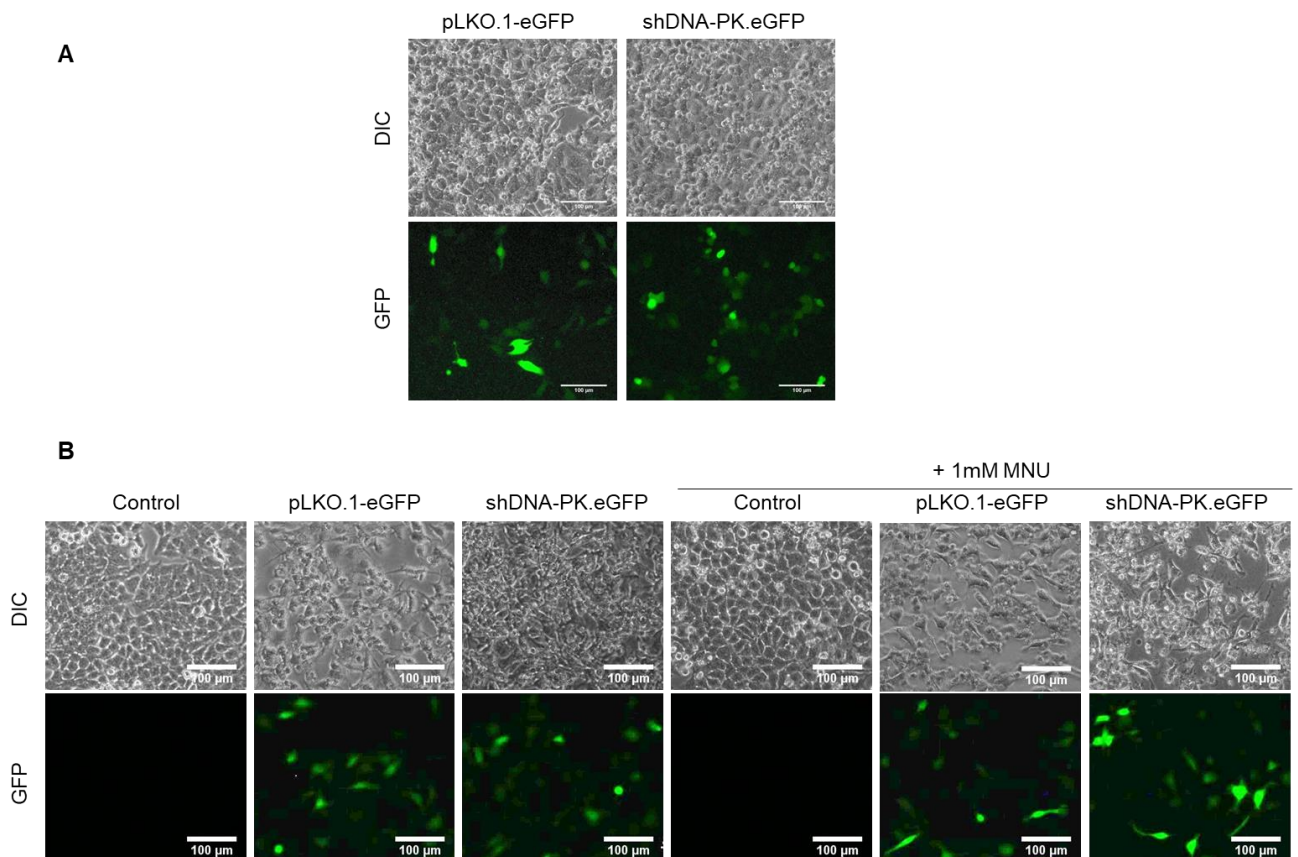
Figure 11: Transfection of shDNA-PK.eGFP in HeLa cells. A) Images for pLKO.1.eGFP and shDNA-PK.eGFP transfected HeLa cells after 24 hours of transfection. **B)** pLKO.1.eGFP and shDNA-PK.eGFP transfected cells after 24 hours of exposure to 1mM MNU induced damage. Scale bar 100 μm.

Immunofluorescence staining for DNA-PKcs

After confirmation of successful transfection, activation of DNA-PK was checked by immunostaining the cells for phospho-DNA-PKcs (T2069). Reduced activation of DNA-PKcs is expected in shDNA-PK.eGFP transfected cells following MNU damage. However, we could not see any significant difference in the activation pattern of DNA-PKcs in shDNA-PK.eGFP transfected cells compared to other MNU treated cells (**Figure 12**)
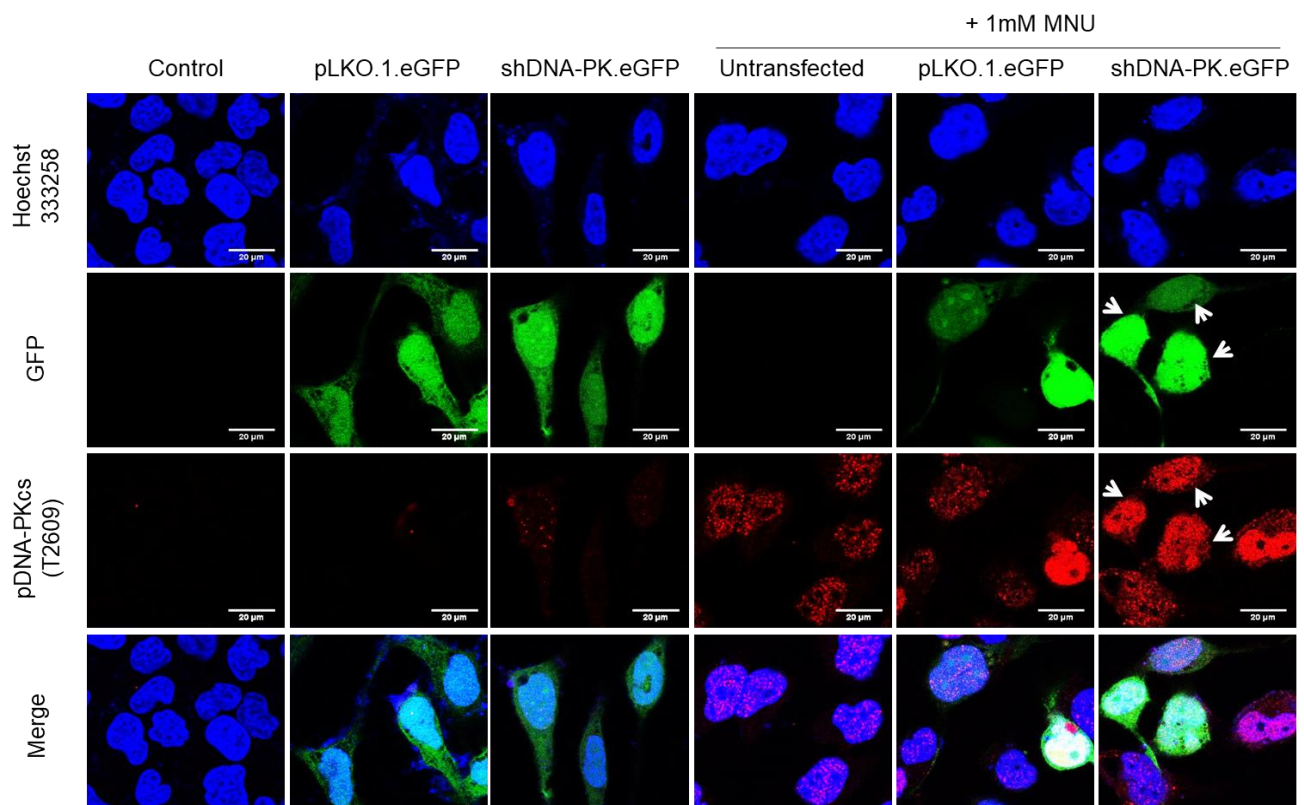

Figure 12: Immunofluorescence image for phospho-DNA-PKcs. IF image for phospho DNA-PKcs (T2069) in shDNA-PK.eGFP transfected HeLa cells upon MNU damage. Hoechst 333258 stains for the nucleus (Blue), GFP for GFP (Green) and phosphoDNA-PKcs for activated DNA-PKcs (Red). Scale bar 20μm

Immunoblotting to check knockdown efficiency of shRNA construct

Since Immunofluorescence (**Figure 12**) did not show any reduction in activation of DNA-PKcs by shRNA mediated knockdown, we decided to check the protein expression levels by western blotting. HeLa cells were seeded in a 60mm dish and transfected with either shDNA-PK.eGFP or empty vector pLKO.1.eGFP by the Lipofectamine-OptiMEM method. Successful transfection was confirmed by 21 hours post-transfection (**Figure 13A**) and cell lysates were collected in 2x sample buffer 48 hours post-transfection.

The cell lysates were run on a 6 % SDS-PAGE and the level of DNA-PKcs (469kDa) was checked using Western blotting. Here, GAPDH (37 kDa) was used as a loading control. No change in the levels of DNA-Pkcs was observed upon transfection of shDNA-PK (**Figure 13B**).
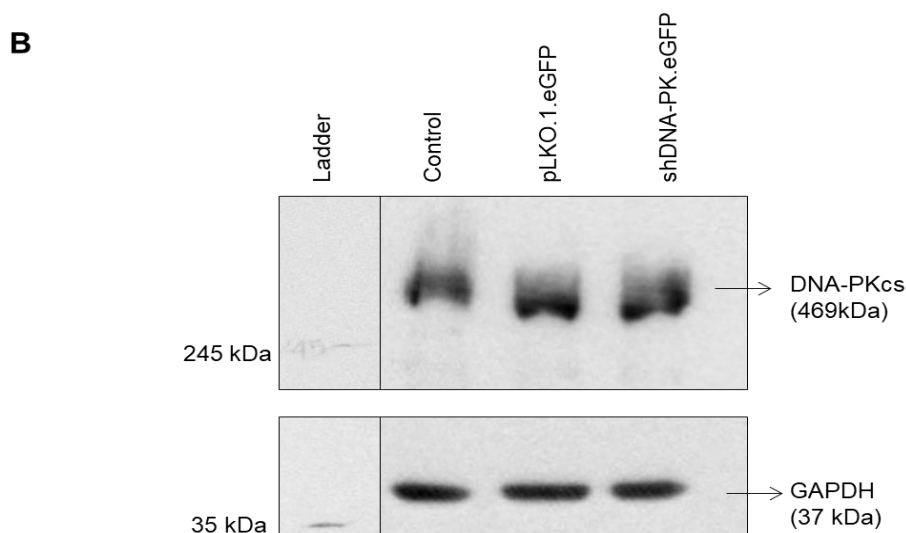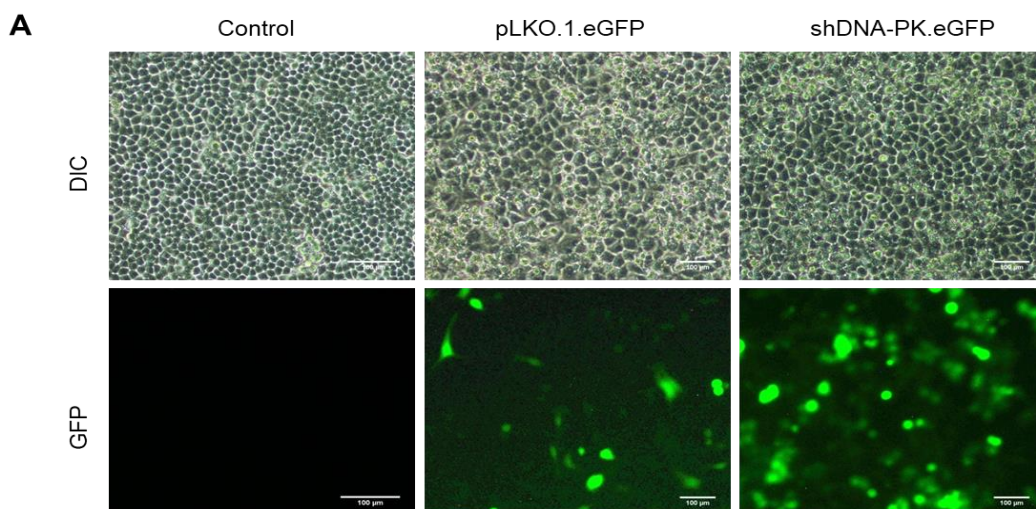
Figure 13: Western blot for DNA-PKcs to check shRNA mediated knockdown. A) Control (untransfected), pLKO.1.eGFP (empty vector) transfected and shDNA-PK.eGFP transfected HeLa cells. Scale bar 100 μm. **B)** Western blot probed for DNA-PKcs (run on 6% resolving gel) and GAPDH as a loading control.

Cloning of shRNA against DNA-PK and checking knockdown

Cloning of shRNA construct against DNA-PK in pLKO.1-TRC vector

From the previous experiments, it is clear that shRNA construct against DNA-PKcs did not show an effective gene silencing. Therefore, we designed new shRNA oligonucleotides and decided to clone it into pLKO.1-TRC cloning vector **(Figure 14A)**. The empty vector was purified using QIAspin miniprep kit and the integrity of purified plasmid was tested on a 0.8% agarose gel (**Figure 14B**).
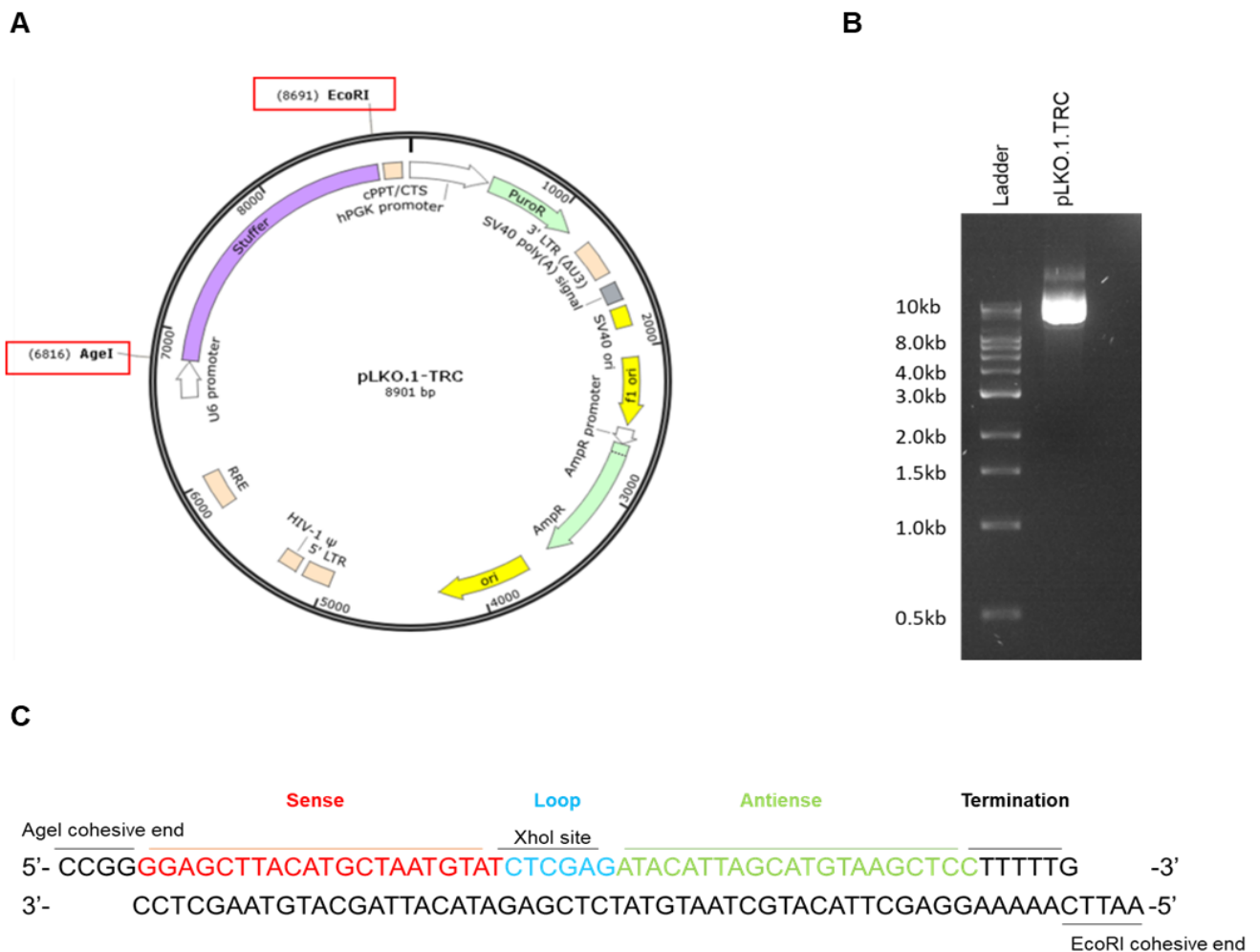
Figure 14: pLKO.1.TRC vector and shRNA construct against DNA-PK. A) Vector map of pLKO.1-TRC with AgeI and EcoRI sites highlighted. Image generated using Snap gene. **B)** 0.8% agarose gel image of the plasmid vector. **C)** shRNA construct against DNA-PKcs

The new shRNA oligonucleotide was designed in such a way that it targets the catalytic domain of DNA-PKcs. The construct has the shRNA sense sequence flanked by AgeI cohesive end (CCGG) at the 5' end of forward oligonucleotide and an EcoRI cohesive end (AATT) at the 5' end of reverse oligonucleotide as shown below. A XhoI site is present in the loop region of the construct (**Figure 14C**).

The stuffer region of 1.9 kb DNA fragment in the pLKO.1-TRC vector was released by double digesting with AgeI and EcoRI (**Figure 15A**). The vector backbone of 7kb was extracted and purified from the gel. Forward and reverse shRNA oligonucleotides were annealed by PCR and loaded on a 3% agarose gel. It yielded a 1:1 ratio of annealed and non-annealed oligonucleotides and annealed band corresponds to 58bp was extracted from the gel (**Figure 15B)**.
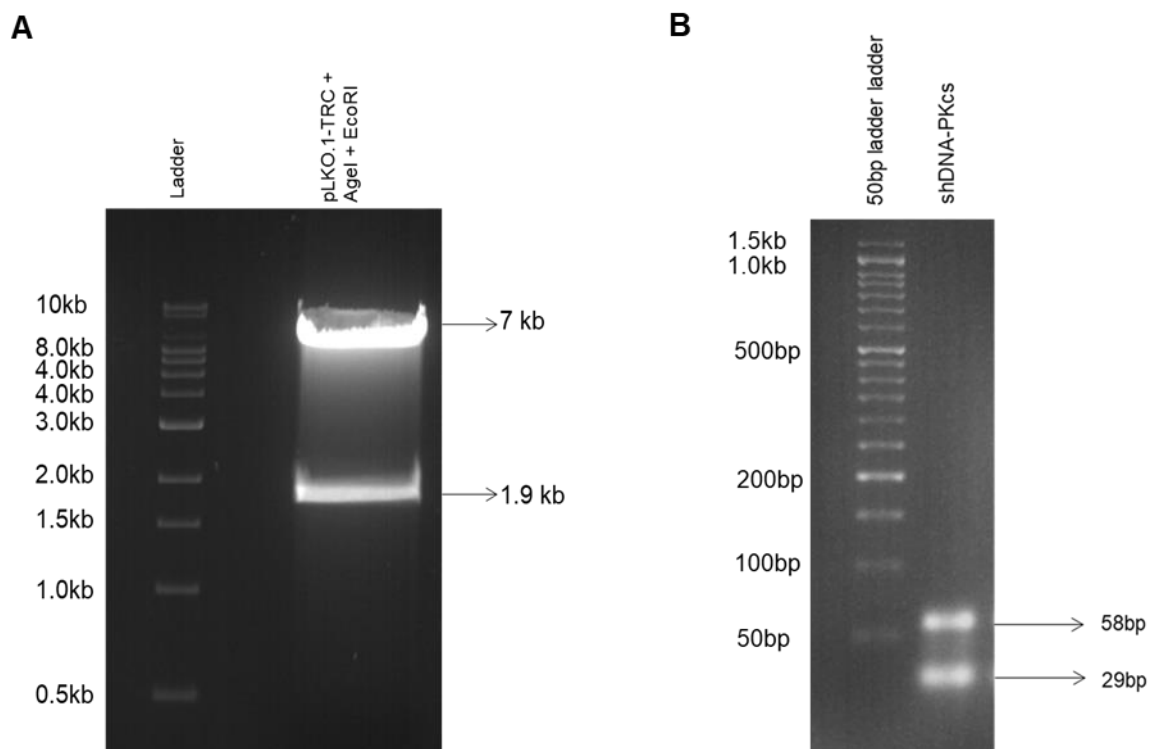

Figure 15: Digested vector and annealed oligonucleotides. A) Empty vector digested with AgeI and EcoRI run on a 1% agarose gel image showing the release of stuffer band

at 1.9 kb. **B)** 3% agarose gel image showing the equal proportion of annealed and non-annealed shRNA oligonucleotides against DNA-PKcs.

Screening for positive clones by XhoI digestion

The annealed oligonucleotides were ligated into the digested vector with 1:1, 1:2, 1:3, 1:4 and 1:5 ratios of vector to insert DNA concentrations and then transformed into *E. coli* DH5α chemically competent cells. We could obtain bacterial colonies in 1:5 ligation plate after transformation. Single colonies were inoculated and the recombinant plasmid was isolated (**Figure 16A**). To confirm successful insertion of the shRNA construct, XhoI digestion was performed since the insert has a XhoI site.

Upon XhoI digestion a release band below 190 bp was observed in all the six recombinant plasmids indicating that these plasmids have the insert of interest and cloning was successful (**Figure 16B**). To further confirm successful insertion of shRNA construct, samples were sent for sequencing.
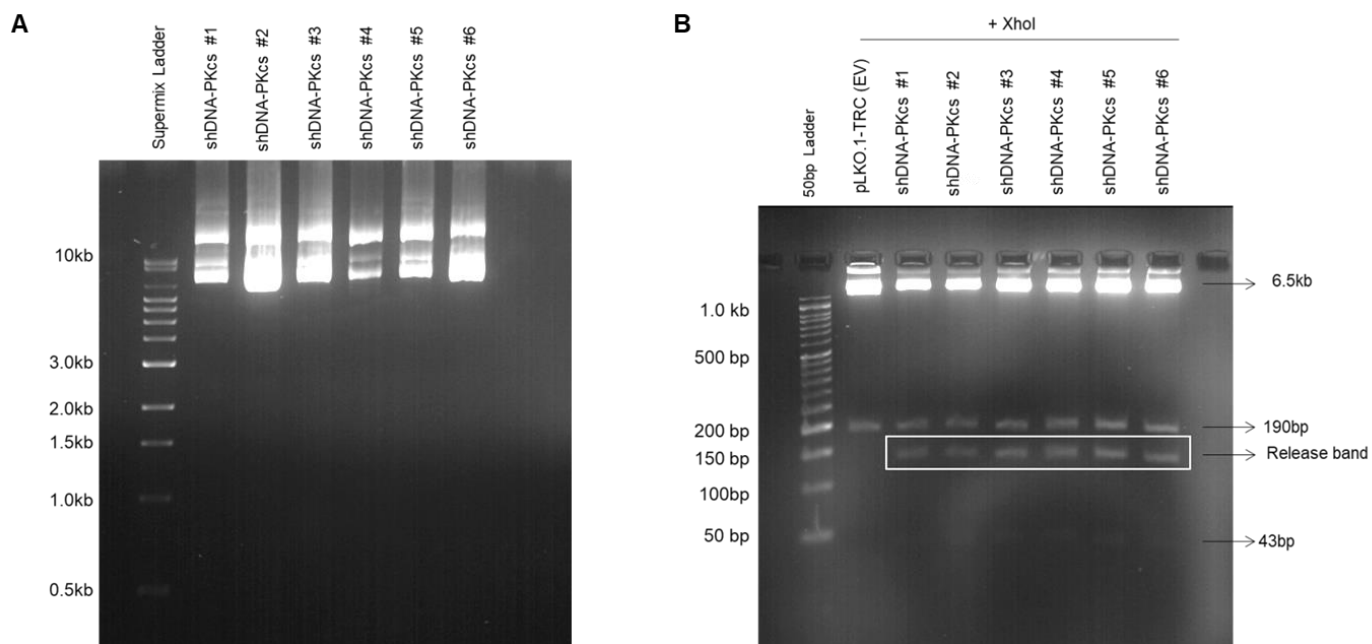

Figure 16: Screening for cloned plasmid by XhoI digestion. A) 0.8% agarose gel image for the recombinant plasmid which was extracted using Miniprep kit. **B)** 2% agarose gel image to analyze digested plasmid upon XhoI digestion showing a release band.

Testing knockdown efficiency of shDNA-PKcs clones in pLKO.1-TRC-shDNA-PKcs transfected HeLa cells

HeLa cells were transfected with 6 of the shDNA-PKcs positive clones obtained in order to test the knockdown efficiency. Cells were seeded in a 24 well plate and transfected with the plasmid containing shDNA-PKcs construct. To select the transfection positive cells a puro selection was performed by treating the cells with optimal dose (0.5µg/ml) of puromycin since the vector has a puromycin resistance gene (**Figure 17A**).
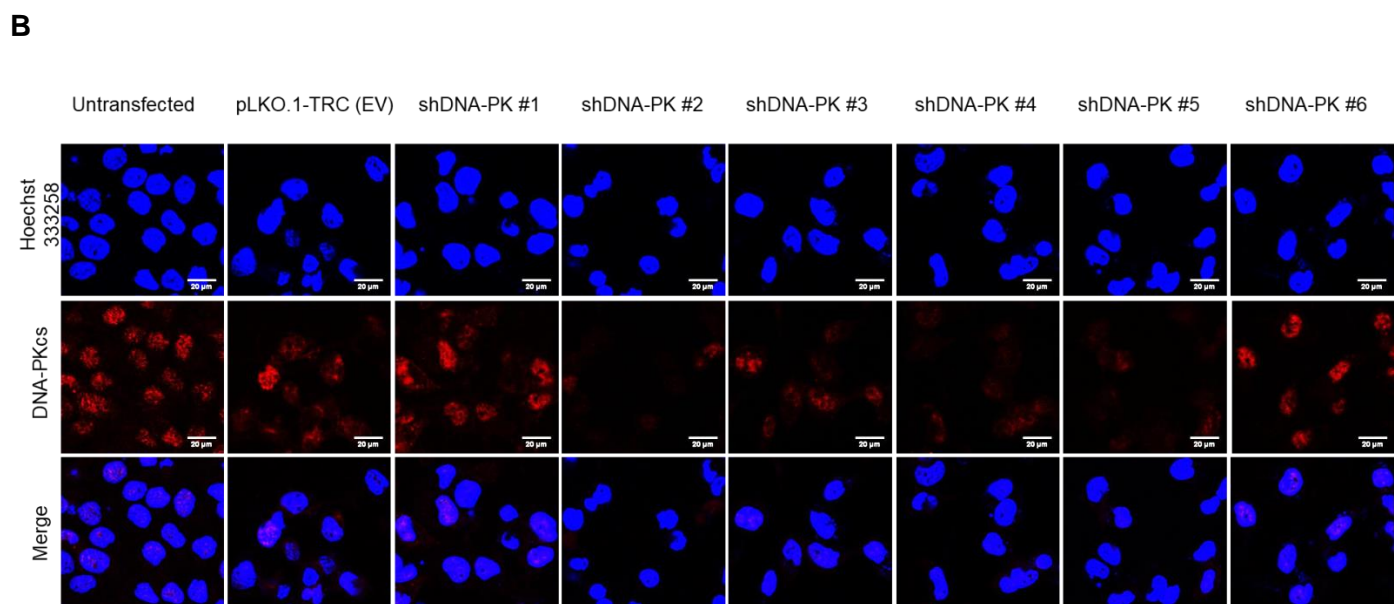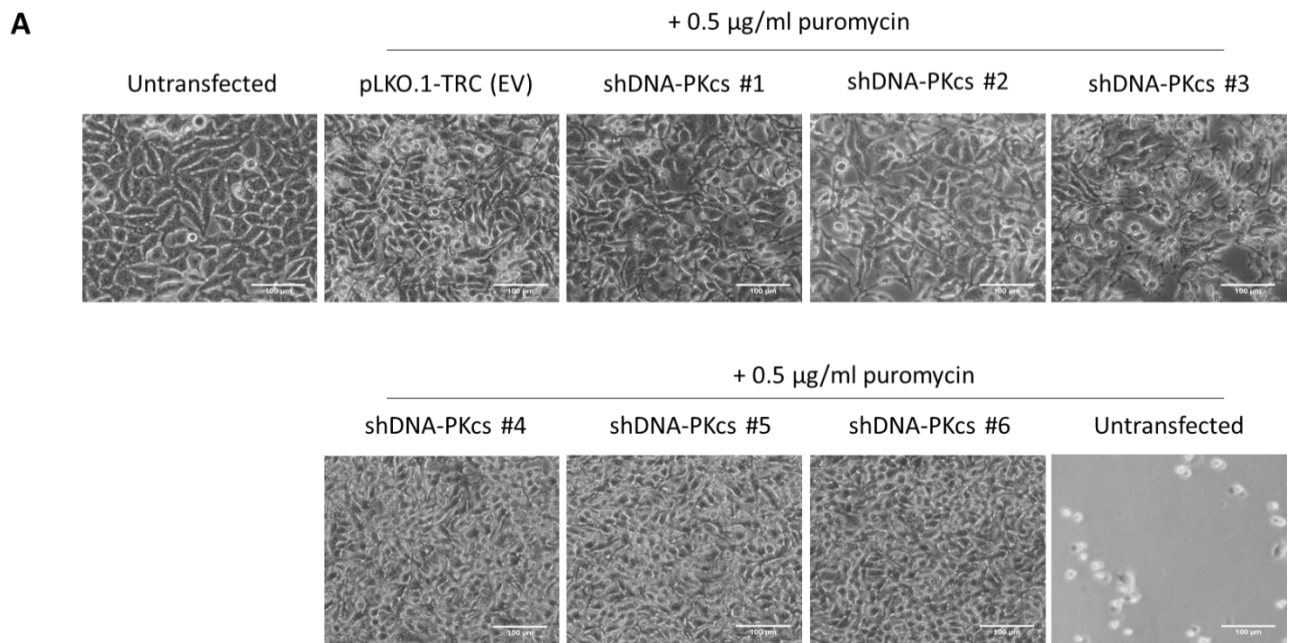
Figure 17: Testing knockdown efficiency of shRNA clones in shDNA-PKcs transfected HeLa cells. A) DIC images for control, pLKO.1-TRC (Empty vector) transfected and shRNA clones transfected HeLa cells after selection with puromycin (0.5µg/ml). Selection was successful as the untransfected cells showed a complete cell death after puromycin treatment. **B)** Immunostained images stained for DNA-PKcs (red) in control, pLKO.1-TRC (Empty vector) transfected and shRNA clones transfected HeLa cells after puromycin selection Compared to control and Empty vector transfected cells, shDNA-PKcs #2, shDNA-PKcs #4 and shDNA-PKcs #5 showed a downregulation of DNA-PKcs. Hoechst 333258 stains the nucleus. Scale bar 20µm.

Selection was done for two days till the untransfected cells showed a complete cell death upon puromycin teatment and cells were fixed and staind for DNA-PKcs. An efficient reduction in DNA-PKcs levels were observed in cells transfected with clones #2, #4 and #5 (**Figure 17 B**) and these clones will be chosen for further experiments. Also the knockdown efficiency will be further confirmed by immunoblotting.

Summary

The aim of this study was to investigate the role of DNA-PK in breast cancer. This study involved analysis of DNA-PK transcript level expression of breast cancer patients using The Cancer Genome Atlas (TCGA) dataset. We could observe a higher expression of DNA-PKcs and Ku80 in tumor tissues compared to adjacent normal tissues of breast cancer and the trend was consistent in all the clinicopathological parameters such as different subtypes, receptor statuses and stages. Moreover, a survival analysis carried out using KM plotter showed a poor survival of breast cancer patients associated with expressing high DNA-PKcs. Taken these result together DNA-PKcs levels were high in breast cancers with more aggressiveness, higher grade and no receptors and it associates with poor survival of patients, implying that DNA-PKcs might play an important role in breast cancer.

We observed an activation of DNA-PKcs at S2056 phosphorylation site in different pre-malignant (MCF10AT1), malignant (MCF10CA1a) and breast cancer cells (MCF7 and T47D). Also aberrant Golgi phenotypes were observed in these cells which are similar to the Golgi dispersal observed in MCF10A treated with MNU upon DNA-PK activation. To identify if it is through DNA-PK, we decided to downregulate DNA-PK by shRNA-mediated knockdown. To genetically silence DNA-PK, we had constructed a shRNA against the catalytic subunit of DNA-PKcs, and three of the tested constructs showed an expected knockdown. Knockdown efficiency of these shRNA constructs will be further confirmed by western blotting and the one which shows maximum knockdown will be chosen for further experiments. Also, a stable DNA-PKcs knockdown MCF10A cell line has to be generated to validate the MNU-induced transformation upon DNA-PK activation using shDNA-PKcs.

References

Abraham, R. T. (2001). "Cell cycle checkpoint signaling through the ATM and ATR kinases." Genes Dev 15(17): 2177-2196.

Anandi, L., et al. (2017). "DNA-PK plays a central role in transformation of breast epithelial cells following alkylation damage." J Cell Sci.

Beskow, C., et al. (2009). "Radioresistant cervical cancer shows upregulation of the NHEJ proteins DNA-PKcs, Ku70 and Ku86." Br J Cancer 101(5): 816-821.

Bouchaert, P., et al. (2012). "DNA-PKcs expression predicts response to radiotherapy in prostate cancer." Int J Radiat Oncol Biol Phys 84(5): 1179-1185.

Burma, S., et al. (2006). "Role of non-homologous end joining (NHEJ) in maintaining genomic integrity." DNA Repair 5(9-10): 1042-1048.

Chaney, S. G. and A. Sancar (1996). "DNA repair: enzymatic mechanisms and relevance to drug response." J Natl Cancer Inst 88(19): 1346-1360.

Ciszewski, W. M., et al. (2014). "DNA-PK inhibition by NU7441 sensitizes breast cancer cells to ionizing radiation and doxorubicin." Breast Cancer Res Treat 143(1): 47-55.

Corominas, M., et al. (1991). "Differential expression of the normal and mutated K-ras alleles in chemically induced thymic lymphomas." Cancer Res 51(19): 5129-5133.

Cox, R. and C. C. Irving (1976). "Effect of N-methyl-N-nitrosourea on the DNA of rat bladder epithelium." Cancer Res 36(11 Pt 1): 4114-4118.

Damia, G. and M. D'Incalci (1998). "Mechanisms of resistance to alkylating agents." Cytotechnology 27(1-3): 165-173.

Davis, A. J. and D. J. Chen (2013). "DNA double strand break repair via non-homologous end-joining." Translational Cancer Research 2(3): 130-143.

Farber-Katz, S. E., et al. (2014). "DNA damage triggers Golgi dispersal via DNA-PK and GOLPH3." Cell 156(3): 413-427.

Fu, D., et al. (2012). "Balancing repair and tolerance of DNA damage caused by alkylating agents." Nat Rev Cancer 12(2): 104-120.

Gates, K. S. (2009). "An overview of chemical processes that damage cellular DNA: spontaneous hydrolysis, alkylation, and reactions with radicals." Chem Res Toxicol 22(11): 1747-1760.

Ghosal, G. and J. Chen (2013). "DNA damage tolerance: a double-edged sword guarding the genome." Transl Cancer Res 2(3): 107-129.

Goodwin, J. F. and K. E. Knudsen (2014). "Beyond DNA repair: DNA-PK function in cancer." Cancer Discov 4(10): 1126-1139.

Goodwin, J. F., et al. (2015). "DNA-PKcs-Mediated Transcriptional Regulation Drives Prostate Cancer Progression and Metastasis." Cancer Cell 28(1): 97-113.

Hamilton, J. T., et al. (2003). "Chloride methylation by plant pectin: an efficient environmentally significant process." Science 301(5630): 206-209.

Hazra, J., et al. (2017). "Engagement of Components of DNA-Break Repair Complex and NFkappaB in Hsp70A1A Transcription Upregulation by Heat Shock." <u>PLoS One</u> 12(1): e0168165.

Hefferin, M. L. and A. E. Tomkinson (2005). "Mechanism of DNA double-strand break repair by non-homologous end joining." <u>DNA Repair (Amst)</u> 4(6): 639-648.

Kastan, M. B. (2008). "DNA damage responses: mechanisms and roles in human disease: 2007 G.H.A. Clowes Memorial Award Lecture." <u>Mol Cancer Res</u> 6(4): 517-524.

Kim, C. H., et al. (2002). "A targeted inhibition of DNA-dependent protein kinase sensitizes breast cancer cells following ionizing radiation." <u>J Pharmacol Exp Ther</u> 303(2): 753-759.

Kotula, E., et al. (2015). "DNA-PKcs plays role in cancer metastasis through regulation of secreted proteins involved in migration and invasion." <u>Cell Cycle</u> 14(12): 1961-1972.

Lanczky, A., et al. (2016). "miRpower: a web-tool to validate survival-associated miRNAs utilizing expression data from 2178 breast cancer patients." <u>Breast Cancer Res Treat</u> 160(3): 439-446.

Lee, S. H. and C. H. Kim (2002). "DNA-dependent protein kinase complex: a multifunctional protein in DNA repair and damage checkpoint." <u>Mol Cells</u> 13(2): 159-166.

Lovejoy, C. A. and D. Cortez (2009). "Common mechanisms of PIKK regulation." <u>DNA Repair (Amst)</u> 8(9): 1004-1008.

Marechal, A. and L. Zou (2013). "DNA damage sensing by the ATM and ATR kinases." <u>Cold Spring Harb Perspect Biol</u> 5(9).

Margison, G. P. and M. F. Santibanez-Koref (2002). "O6-alkylguanine-DNA alkyltransferase: role in carcinogenesis and chemotherapy." <u>Bioessays</u> 24(3): 255-266.

Matsuoka, S., et al. (1998). "Linkage of ATM to cell cycle regulation by the Chk2 protein kinase." <u>Science</u> 282(5395): 1893-1897.

Menke, M., et al. (2000). "N-Methyl-N-nitrosourea-induced DNA damage detected by the comet assay in Vicia faba nuclei during all interphase stages is not restricted to chromatid aberration hot spots." <u>Mutagenesis</u> 15(6): 503-506.

Mladenov, E., et al. (2013). "DNA double-strand break repair as determinant of cellular radiosensitivity to killing and target in radiation therapy." <u>Front Oncol</u> 3: 113.

Norbury, C. J. and I. D. Hickson (2001). "Cellular responses to DNA damage." <u>Annu Rev Pharmacol Toxicol</u> 41: 367-401.

Qin, X., et al. (1999). "Transgenic expression of human MGMT blocks the hypersensitivity of PMS2-deficient mice to low dose MNU thymic lymphomagenesis." <u>Carcinogenesis</u> 20(9): 1667-1673.

Reese, J. S., et al. (2001). "Overexpression of human O6-alkylguanine DNA alkyltransferase (AGT) prevents MNU induced lymphomas in heterozygous p53 deficient mice." <u>Oncogene</u> 20(38): 5258-5263.

Shintani, S., et al. (2003). "Up-regulation of DNA-dependent protein kinase correlates with radiation resistance in oral squamous cell carcinoma." <u>Cancer Sci</u> 94(10): 894-900.

Smith, G. C. and S. P. Jackson (1999). "The DNA-dependent protein kinase." <u>Genes Dev</u> 13(8): 916-934.

Stokes, M. P., et al. (2007). "Profiling of UV-induced ATM/ATR signaling pathways." Proc Natl Acad Sci U S A 104(50): 19855-19860.

Takahashi, A., et al. (2014). "Nonhomologous End-Joining Repair Plays a More Important Role than Homologous Recombination Repair in Defining Radiosensitivity after Exposure to High-LET Radiation." Radiat Res 182(3): 338-344.

Torre, L. A., et al. (2015). "Global cancer statistics, 2012." CA Cancer J Clin 65(2): 87-108.

Tsubura, A., et al. (2010). "Animal models for retinitis pigmentosa induced by MNU; disease progression, mechanisms and therapeutic trials." Histol Histopathol 25(7): 933-944.

Um, J. H., et al. (2004). "Relationship between antiapoptotic molecules and metastatic potency and the involvement of DNA-dependent protein kinase in the chemosensitization of metastatic human cancer cells by epidermal growth factor receptor blockade." J Pharmacol Exp Ther 311(3): 1062-1070.

Warwick, G. P. (1963). "The Mechanism of Action of Alkylating Agents." Cancer Res 23: 1315-1333.

Weterings, E. and D. J. Chen (2008). "The endless tale of non-homologous end-joining." Cell Research 18(1): 114-124.

Yu, S., et al. (2017). "The T47D cell line is an ideal experimental model to elucidate the progesterone-specific effects of a luminal A subtype of breast cancer." Biochem Biophys Res Commun 486(3): 752-758.

Zarbl, H., et al. (1985). "Molecular assays for detection of ras oncogenes in human and animal tumors." Carcinog Compr Surv 9: 1-16.

Zhou, B. B. and S. J. Elledge (2000). "The DNA damage response: putting checkpoints in perspective." Nature 408(6811): 433-439.